

Showcasing research from Professor John Gladysz's laboratory, Department of Chemistry, Texas A&M University, College Station, Texas, USA.

Platinum(II) alkyl complexes of chelating dibridgehead diphosphines $P((CH_2)_n)_3P$ ($n = 14, 18, 22$); facile *cis/trans* isomerizations interconverting gyroscope and parachute like adducts

The dibridgehead diphosphines $P((CH_2)_n)_3P$ can serve either as *cis* or *trans* spanning chelate ligands, termed "parachute" and "gyroscope" systems, respectively. This work examines the dependence of the ancillary ligands upon this equilibrium, using both experimental and computational probes. The diphosphines ligands in the *cis* isomers are intrinsically more strained, but they are nonetheless favoured with strong sigma donor ligands such as *n*-alkyl.

As featured in:



See Michael B. Hall, John A. Gladysz et al., *Dalton Trans.*, 2021, **50**, 12457.

PAPER

[View Article Online](#)
[View Journal](#) | [View Issue](#)Cite this: *Dalton Trans.*, 2021, **50**,
12457

Platinum(II) alkyl complexes of chelating dibridgehead diphosphines $P((CH_2)_n)_3P$ ($n = 14, 18, 22$); facile *cis/trans* isomerizations interconverting gyroscope and parachute like adducts†

Yun Zhu,[‡] Andreas Ehnborn,[‡] Tobias Fiedler,[‡] Yi Shu, Nattamai Bhuvanesh, Michael B. Hall[‡] * and John A. Gladysz[‡] *

The gyroscope like dichloride complexes $trans\text{-Pt}(\text{Cl})_2(P((CH_2)_n)_3P)$ ($trans\text{-2}$; $n = \text{c}, 14; \text{e}, 18; \text{g}, 22$) and MeLi (2 equiv.) react to yield the parachute like dimethyl complexes $cis\text{-Pt}(\text{Me})_2(P((CH_2)_n)_3P)$ ($cis\text{-4c,e,g}$, 70–91%). HCl (1 equiv.) and $cis\text{-4c}$ react to give $cis\text{-Pt}(\text{Cl})(\text{Me})(P((CH_2)_{14})_3P)$ ($cis\text{-5c}$, 83%), which upon stirring with silica gel or crystallization affords $trans\text{-5c}$ (89%). Similar reactions of HCl and $cis\text{-4e,g}$ give $cis/trans\text{-5e,g}$ mixtures that upon stirring with silica gel yield $trans\text{-5e,g}$. A parallel sequence with $trans\text{-2c/EtLi}$ gives $cis\text{-Pt}(\text{Et})_2(P((CH_2)_{14})_3P)$ ($cis\text{-6c}$, 85%) but subsequent reaction with HCl affords $trans\text{-Pt}(\text{Cl})(\text{Et})(P((CH_2)_{14})_3P)$ ($trans\text{-7c}$, 45%) directly. When previously reported $cis\text{-Pt}(\text{Ph})_2(P((CH_2)_{14})_3P)$ is treated with HCl (1 equiv.), *cis*- and *trans*- $Pt(\text{Cl})(\text{Ph})(P((CH_2)_{14})_3P)$ are isolated (44%, 29%), with the former converting to the latter at 100 °C. Reactions of $trans\text{-5c}$ and LiBr or NaI afford the halide complexes $trans\text{-Pt}(\text{X})(\text{Me})(P((CH_2)_{14})_3P)$ ($trans\text{-9c}$, 88%; $trans\text{-10c}$, 87%). Thermolyses and DFT calculations that include acyclic model compounds establish *trans* > *cis* stabilities for all except the dialkyl complexes, for which energies can be closely spaced. The σ donor strengths of the non-phosphine ligands are assigned key roles in the trends. The crystal structures of $cis\text{-4c}$, $trans\text{-5c}$, $trans\text{-7c}$, and $trans\text{-10c}$ are determined and analyzed together with the computed structures.

Received 13th July 2021,
Accepted 23rd August 2021

DOI: 10.1039/d1dt02321g

rsc.li/dalton

Introduction

The broad field of molecular rotors is highly relevant to several types of molecular machines, and in lieu of an extensive list of primary research articles, readers are referred to three expansive reviews.^{1–3} We have had an ongoing interest in the sub-nanoscale miniaturization of various macroscopic devices, and this has driven the synthesis and intensive study of two classes of metal complexes in our group. The first, exemplified by *trans*-II in Scheme 1, has been termed “gyroscope like” due to the obvious geometric resemblance.³ Such species can be accessed *via* three-fold ring closing metathesis/hydrogenation sequences involving complexes with *trans* phosphine ligands of the formula $P((CH_2)_mCH=CH_2)_3$ (*trans*-I).^{3–7} This affords adducts of cage like dibridgehead diphosphines with three

connecting $(CH_2)_n$ bridges ($n = 2m + 2$). Depending upon the lengths of the methylene segments and the sizes of the ligands, the ML_2 rotators may be capable of rotation, exchanging the positions of the ligands or (equivalently) the $(CH_2)_n$ bridges.

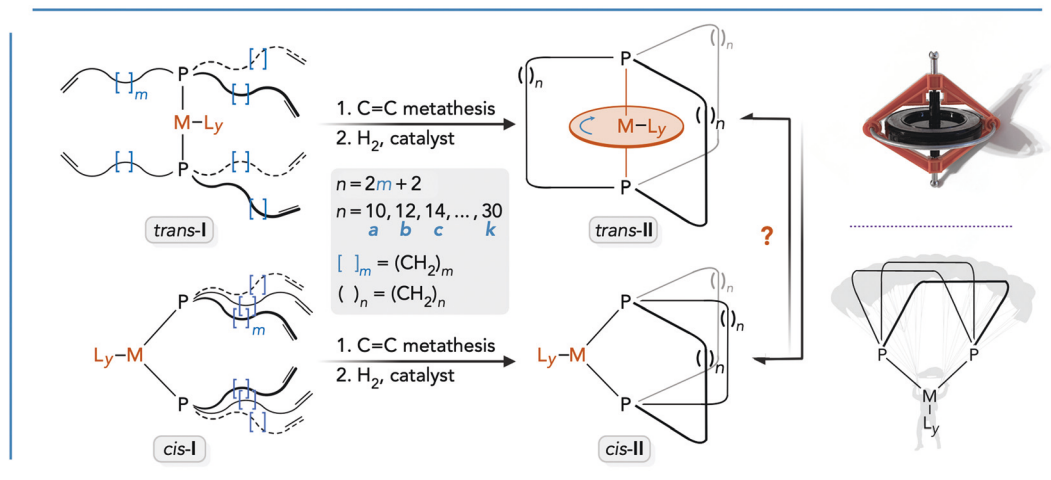
When such sequences are carried out with analogous *cis* complexes (e.g., *cis*-I, Scheme 1), the same diphosphine ligands can be generated, but now with the donor atoms connecting *cis* positions.⁸ When accessed in square planar geometries, one $(CH_2)_n$ bridge can be visualized as lying in the coordination plane, the second above, and the third below. Depending upon the lengths of the methylene segments and the sizes of the ligands, the bridges may be capable of “jump rope” dynamic processes that exchange their positions. When square planar versions of *cis*-II are viewed from appropriate perspectives, there is some resemblance to a parachutist, so they are often termed “parachute like”.

In analyzing the dynamic behavior of both classes of complexes, it has been important to exclude alternative mechanisms for exchanging the positions of ligands or $(CH_2)_n$ bridges.⁹ Specifically, any facile *trans/cis* isomerization could open up new pathways. In one embodiment, gyroscope like *trans*-II might first undergo a hypothetically endergonic iso-

Department of Chemistry, Texas A&M University, PO Box 30012, College Station, Texas 77842-3012, USA. E-mail: gladysz@mail.chem.tamu.edu, mbhall@tamu.edu

† Electronic supplementary information (ESI) available: Additional crystallographic and computational data. CCDC 2064494, 2067661, 2067664 and 2070891. For ESI and crystallographic data in CIF or other electronic format see DOI: 10.1039/d1dt02321g

‡ Deceased 28 October 2020.



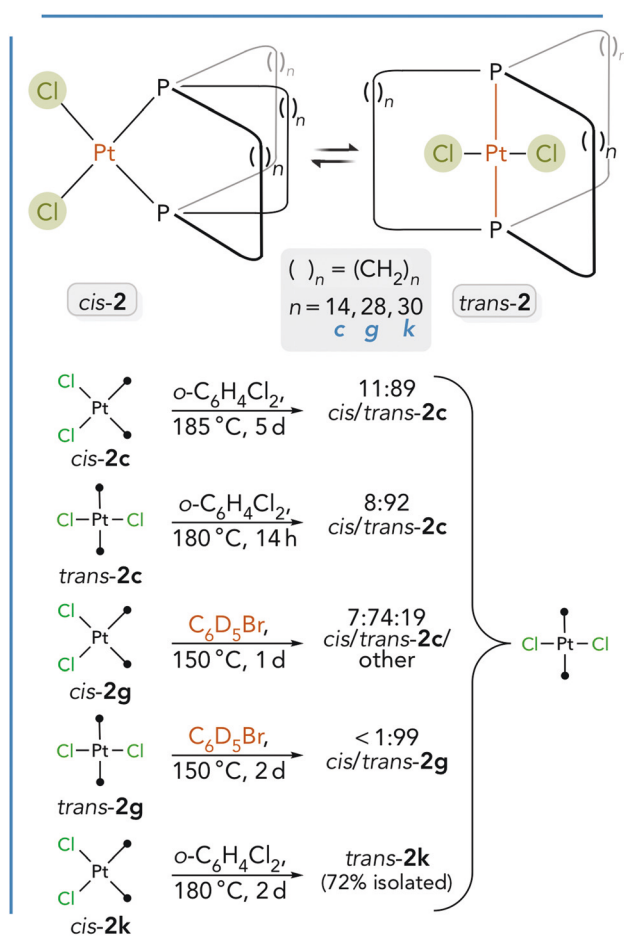
Scheme 1 Generalized syntheses of gyroscope like (*trans*-II) and parachute like (*cis*-II) metal complexes.

merization to parachute like *cis*-II, where $(\text{CH}_2)_n$ exchange might be more rapid than in *trans*-II ("jump rope" rate > ML_y rotation). Alternatively, one can play the devil's advocate in the opposite direction. Thus, we have sought to probe the relative stabilities of *cis/trans*-II and their thermal interconversion both experimentally and computationally.

In earlier studies, we examined these issues with a series of platinum dichloride complexes, *cis*- and *trans*-Pt(Cl)₂P((CH_2)_n)₃P (*cis*- and *trans*-2).^{4c,8} As shown in Scheme 2, temperatures of 150–185 °C were required to effect equilibrations on reasonable time scales from either direction. In all cases, the gyroscope like *trans* isomers were favored. To facilitate comparisons with earlier papers, the same letter indices have been employed for *n* (*n* = 10, **a**; 12, **b**; 14, **c**; etc.). Computationally, as one goes from $(\text{CH}_2)_{10}$ (**2a**) to $(\text{CH}_2)_{22}$ (**2g**), or 13- to 25-membered macrocycles, the gyroscope like *trans*-2 ranges from 5.1 to 9.2 kcal mol^{−1} more stable than the parachute like *cis*-2.^{8,10}

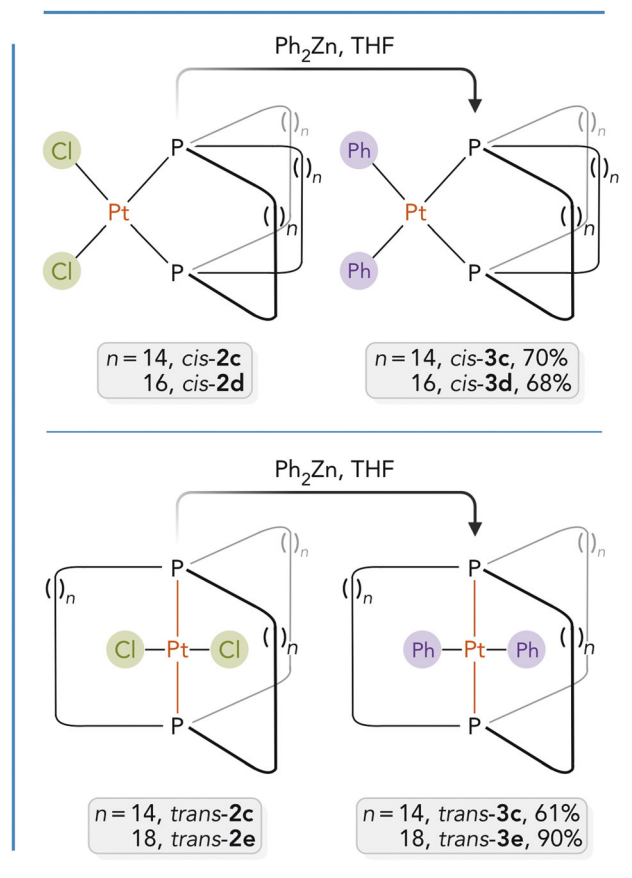
The acyclic precursor complexes *cis*- and *trans*-Pt(Cl)₂P((CH_2)_mCH=CH₂)₃ (*cis*- and *trans*-1) could also be thermally equilibrated.^{4c} Here, in line with literature precedent,^{11,12} there is a significant effect of solvent polarity that tracks the dipole moments (*cis* > *trans*; more polar CH_2Cl_2 : appreciable amounts of both isomers; less polar toluene: >95% *trans*).¹³ Other reactivity data are relevant. As shown in Scheme 3, the dichloride complexes **2** and Ph_2Zn react at room temperature to give the diphenyl complexes Pt(Ph)₂P((CH_2)_n)₃P (**3**).⁴ Since *cis*-**2c,d** and *trans*-**2c,e** afford *cis*-**3c,d** and *trans*-**3c,e**, respectively, these fit the textbook definition of stereospecific reactions.¹⁴ Furthermore, the stereospecificity excludes *cis/trans* isomerization at any stage of the reaction coordinates.

In this paper, we report the surprising observation of much lower energy pathways for the interconversion of *trans*-II and *cis*-II when the chloride ligands in **2** are replaced by one or more alkyl groups. Since these isomerizations impinge upon a number of mechanistic questions, even beyond those



Scheme 2 Previously studied isomerizations of parachute and gyroscope like complexes.

expressed above, it was imperative to bring definition to the phenomena. Accordingly, a variety of synthetic, structural, thermolytic, and computational experiments have been carried



Scheme 3 Stereospecific substitution of chloride ligands by phenyl ligands in *trans* and *cis* platinum complexes.

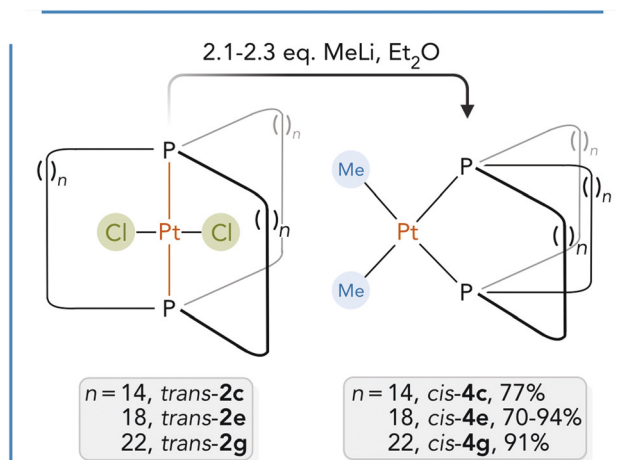
out, as detailed in the narrative below. None of these data have been previously communicated.

Results

Syntheses and NMR characterization

As shown in Scheme 4, the gyroscope like platinum dichloride complexes *trans*-**2c,e,g**^{4a} were treated with diethyl ether solutions of MeLi (2.1–2.3 equiv.). Workups gave the new parachute like dimethyl complexes *cis*-Pt(Me)₂(P((CH₂)_n)₃P) (*cis*-**4c,e,g**) in 70–94% yields as air stable white solids. When the first such reaction was conducted, the *trans/cis* isomerization was considered surprising. Thus, the neutral alumina columns used in initial experiments were omitted. However, identical results were obtained.

These and all other new complexes below were characterized by NMR spectroscopy (¹H, ¹³C{¹H}, ³¹P{¹H}) and microanalyses, as summarized in the Experimental section. The *cis* stereochemistry was evidenced by a number of features, such as the lower ¹J_{Pt} values (1853–1886 Hz vs. 2389–2398 Hz for *trans*-**2c,e,g**).¹⁵ Each ¹³C{¹H} NMR spectrum showed a doublet of doublets for the methyl groups (²J_{CP(*trans*)} = 101.7–101.1 Hz, ²J_{CP(*cis*)} = 9.9–10.0 Hz). Each ¹H NMR spectrum also showed a



Scheme 4 Substitution of the chloride ligands in *trans*-**2c,e,g** by methyl ligands with isomerization.

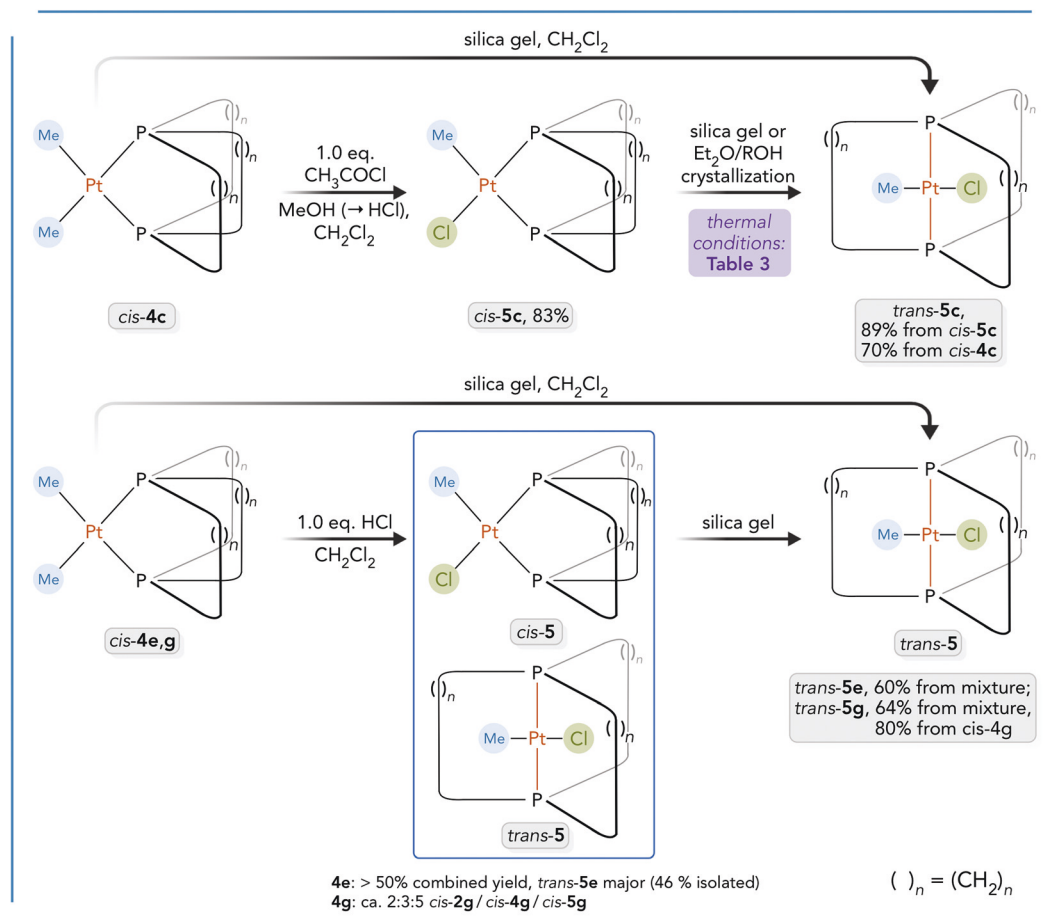
doublet of doublets (³J_{HP(*trans*)} = 7.3–6.7 Hz, ³J_{HP(*cis*)} = 6.1–5.7 Hz), and platinum satellites were usually visible (²J_{HPT} = 66–65 Hz). The ¹H and ³¹P NMR properties were very similar to those reported for the related acyclic complexes *cis*-Pt(Me)₂(PR₃)₂.^{16,17}

A reaction of *trans*-**2c** and only 1.1 equiv. of MeLi was similarly conducted. A ³¹P{¹H} NMR spectrum of the crude reaction mixture showed 40–50% conversion to the dimethyl complex *cis*-**4c**. The only other signal detected was that of the starting material *trans*-**2c**. Thus, it was not possible to interrogate the stereochemistry of the presumed intermediate, the methyl chloride complex Pt(Cl)(Me)(P((CH₂)₁₄)₃P) (**5c**). When the reaction of *trans*-**2c** and 2.2 equiv. of MeLi (Scheme 4) was repeated at 0 °C, the result was the same as at room temperature.

As shown in Scheme 5, CH₂Cl₂ solutions of *cis*-**4c,e,g** were treated with 1.0 equiv. of HCl. In some cases the HCl was generated *in situ* from acetyl chloride (1.0 equiv.) and excess methanol, and in other cases 2.0 M Et₂O solutions were used. With *cis*-**4c**, a chromatographic workup (neutral alumina) gave parachute like *cis*-Pt(Cl)(Me)(P((CH₂)₁₄)₃P) (*cis*-**5c**) in 83% yield. The lower symmetry was evidenced by doubled ³¹P NMR signals, and PtCH₃ ¹H and ¹³C NMR signals that were now doublets of doublets. Analogous patterns have been noted for the related complexes *cis*-Pt(Cl)(Me)(PR₃)₂.^{17,18}

The stereochemical homogeneity of *cis*-**5c** was quickly found to be tied to a hair trigger. Either exposure to silica gel (in the form of a column or slurry) or crystallization (Et₂O/methanol or Et₂O/ethanol) afforded gyroscope like *trans*-**5c** (≥89%). Even CH₂Cl₂ solutions of the dimethyl complex *cis*-**4c**, when slurried with silica gel, gave *trans*-**5c** (70%). The NMR properties of *trans*-**5c** were similar to those of the dichloride complex *trans*-**2c**, with the ¹H and ¹³C NMR spectra showing triplets for the PtCH₃ group.

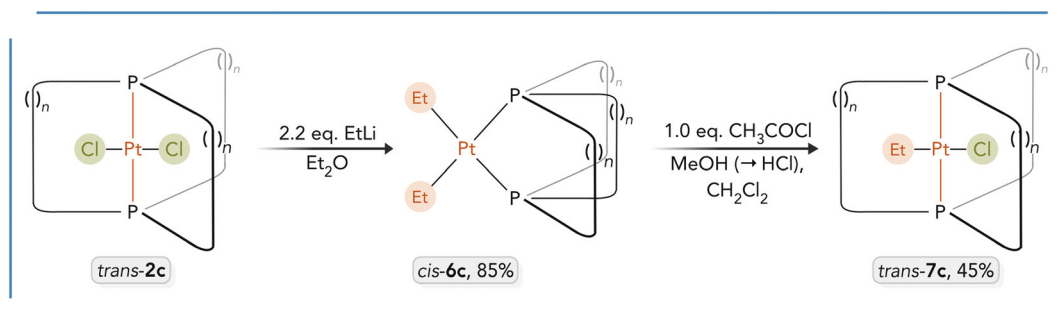
With *cis*-**4e,g**, the analogous methyl chloride complexes *cis*-**5e,g** could be detected “on the fly”, but isolated samples always contained significant amounts of *trans*-**5e,g**. These mix-



Scheme 5 Introduction of halide ligands and attendant isomerization.

tures were further slurried with silica gel to give pure *trans-5e*, *g* (60–64%). Additional details can be found in the Experimental section. The NMR properties were similar to those of *trans-5c*, and all three complexes exhibited $^1J_{\text{Pt}}$ values (2824–2796 Hz) that were diagnostic of the *trans* stereochemistry.¹⁵ Given the modest dependence of the chemistry in Schemes 3–5 upon the lengths of the $(\text{CH}_2)_n$ bridges, subsequent experiments were confined to $(\text{CH}_2)_{14}$ systems (“c series”).

As depicted in Scheme 6, a parallel sequence was carried out with *trans-2c* and EtLi in place of MeLi . The parachute like diethyl complex *cis-Pt*(Et)₂ $\text{P}((\text{CH}_2)_{14})_3\text{P}$ (*cis-6c*) was isolated in 85% yield. NMR spectra showed a $^1J_{\text{Pt}}$ value of 1746 Hz, and PtCH_2CH_3 ^1H signal patterns similar to those of related acyclic complexes *cis-Pt*(Et)₂(PR_3)₂.¹⁶ Next, *cis-6c* was treated with HCl analogously to the dimethyl complex *cis-4c* in Scheme 5. However, the same chromatographic workup (neutral alumina) afforded only gyroscope like *trans-7c* (45%). Accordingly, the



Scheme 6 Substitution and isomerization reactions involving ethyl ligands.

NMR spectra now showed a $^1J_{\text{Pt}}$ value of 3002 Hz, and PtCH_2CH_3 ^1H signal patterns similar to those of other complexes of the type $\text{trans-Pt}(\text{Cl})(\text{Et})(\text{PR}_3)_2$.¹⁹ No significant amounts of byproducts were noted when crude reaction mixtures were assayed by ^{31}P NMR.

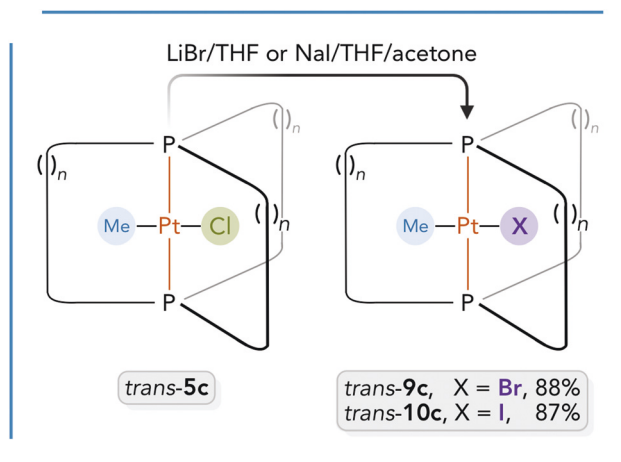
The main difference between the substitution reactions of the gyroscope like dichloride complex trans-2c in Schemes 4 and 6 and that in Scheme 3 is the use of alkyl lithium *versus* aryl zinc nucleophiles. Thus, as shown in Scheme 7 (top), trans-2c was treated with PhLi in a procedure analogous to that in Scheme 6. Workup gave the gyroscope like diphenyl complex trans-3c in 85% yield. All of the syntheses in this report have been reproduced several times, often by different coworkers. However, in one case this same reaction gave, under essentially identical conditions, trans-3c and cis-3c in 50% and 29% isolated yields, respectively. Regardless, the chloride/phenyl ligand substitution is not accompanied by the same degree of isomerization as chloride/alkyl ligand substitution.

In previous work, the gyroscope like diphenyl complexes $\text{trans-Pt}(\text{Ph})_2(\text{P}((\text{CH}_2)_n)_3\text{P})$ (trans-3c,e) had been shown to react with 1.0 equiv. of HCl to give the gyroscope like phenyl chloride complexes $\text{trans-Pt}(\text{Cl})(\text{Ph})(\text{P}((\text{CH}_2)_n)_3\text{P})$ (trans-8c,e) in 93–98% yields after workup. This is exemplified with trans-3c in Scheme 7 (top). However, analogous substitution reactions with parachute like cis-3 had not been investigated. Thus, cis-3c and HCl were similarly combined (Scheme 7, bottom). A chromatographic workup (neutral alumina) gave the easily separated products cis-8c (44%) and trans-8c (29%). The structure of the former, a new compound, followed readily from the types of NMR properties detailed above.

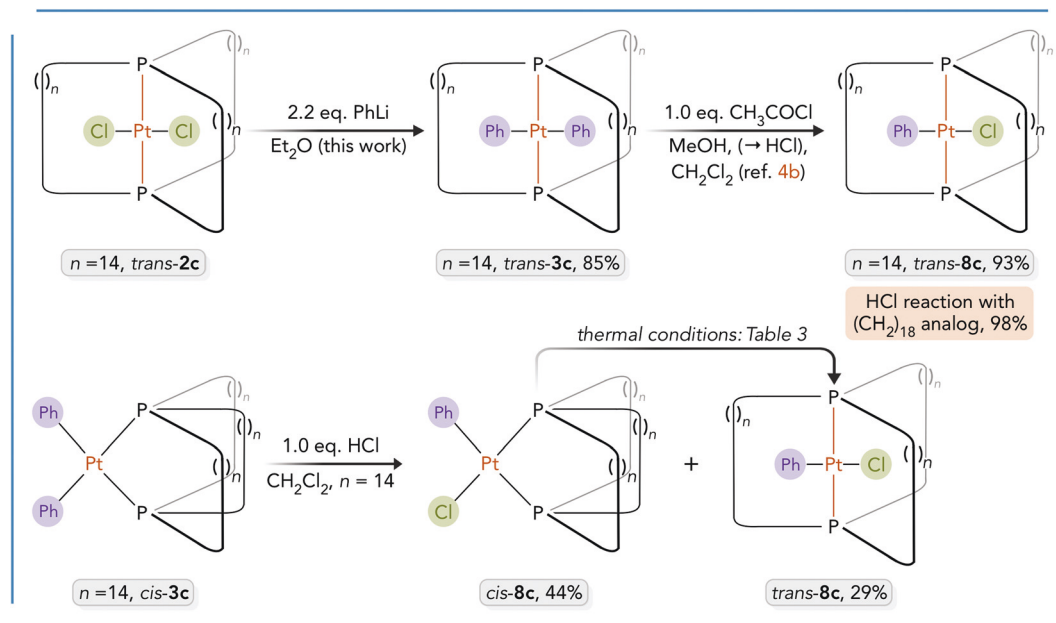
In connection with thermolyses described below, authentic samples of platinum bromide and iodide complexes became of interest. Thus, as shown in Scheme 8, the gyroscope like chloride complex trans-5c was treated (in separate reactions) with LiBr or NaI . Workups gave the gyroscope like halide complexes $\text{trans-Pt}(\text{X})(\text{Me})(\text{P}((\text{CH}_2)_{14})_3\text{P})$ ($\text{X} = \text{Br}$, trans-9c ; Cl , trans-10c) in 87–88% yields. The structure and stereochemistry followed readily from the NMR properties, as well as a crystal structure in the following section.

Crystallographic characterization

Due to the varied stereochemical issues involving the preceding complexes, crystal structures were sought wherever poss-



Scheme 8 Halide substitution reactions.



Scheme 7 Substitution and isomerization reactions involving phenyl ligands.

ible. Single crystals of *cis*-**4c**, *trans*-**5c**, *trans*-**7c**, and *trans*-**10c** could be obtained, and the X-ray structures were determined as described in the Experimental section and Table 1. Key metrical parameters are summarized in Table 2. Thermal ellipsoid plots are depicted in Fig. 1–4. All of the structures exhibited disorder that could easily be modeled (Me/X positions in *trans*-**5c** and *trans*-**10c**; certain (CH₂)_n segments in *cis*-**4c**, *trans*-**5c**, and *trans*-**7c**). Data are given only for the dominant conformation.

As shown in Fig. 1, the dimethyl complex *cis*-**4c** exhibits, as with other parachute like adducts structurally characterized earlier,⁸ one macrocycle in which the proximal CH₂ groups lie close to the coordination plane, and two in which the proximal CH₂ groups lie in roughly perpendicular planes. With the gyroscope like ethyl chloride complex *trans*-**7c**, three independent molecules were found in the unit cell. Since these involved rather minor conformational differences, only one is depicted in Fig. 3, but all are illustrated in the ESI.†

The views of the iodide complex *trans*-**10c** in Fig. 4 and the analogous chloride complex *trans*-**5c** in Fig. 2 have been arranged as closely as possible. While these adducts clearly pass the “eye test” as isostructural, the space groups are not identical (*Pbca* vs. *P12₁/n1*) and the crystal lattices differ.

Additional characterization of equilibria

Attention was turned to addressing certain gaps in the preceding preparative data. Although the reactions in Scheme 5 convincingly show that for the methyl chloride complexes **5c,e,g**, the *trans*/gyroscope isomers are more stable than the *cis*/parachute isomers, purely thermal conversions of purified samples were lacking. Accordingly, when *o*-C₆H₄Cl₂ or C₆D₅Br solutions of *cis*-**5c** were kept at 100–110 °C for 3–7 h, or toluene solutions kept at 80 °C for 72 h, or mesitylene solutions kept at 140 °C for 0.5 h, >99% conversions to *trans*-**5c** were observed, as assayed by ³¹P{¹H} NMR. These data are from entries 9–13 of Table 3.

The previously reported thermolyses in Scheme 2 unambiguously show that the gyroscope like dichloride complexes *trans*-**2** are more stable than the parachute like *cis*-**2**. Since the procedures for isolating the latter did not involve silica gel (found to promote *cis/trans* isomerization in Scheme 5), it was of interest to see if conversion to *trans*-**2c** might be effected in slurries. However, no reaction occurred when *cis*-**2c** was combined with silica gel for 24 h at room temperature in toluene-*d*₈ or CDCl₃ (entry 1, Table 3).

The workups for isolating the analogous diphenyl complexes *cis*-**3c,d** (Scheme 3) did involve silica gel.⁸ Nonetheless,

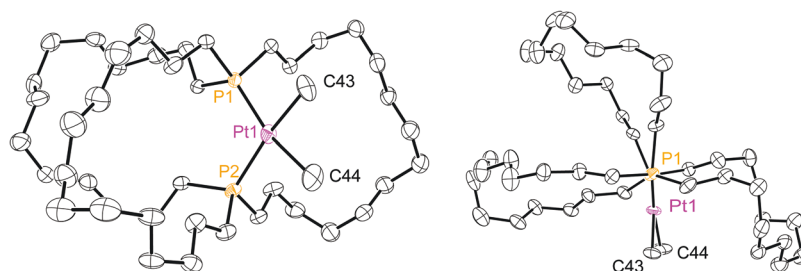
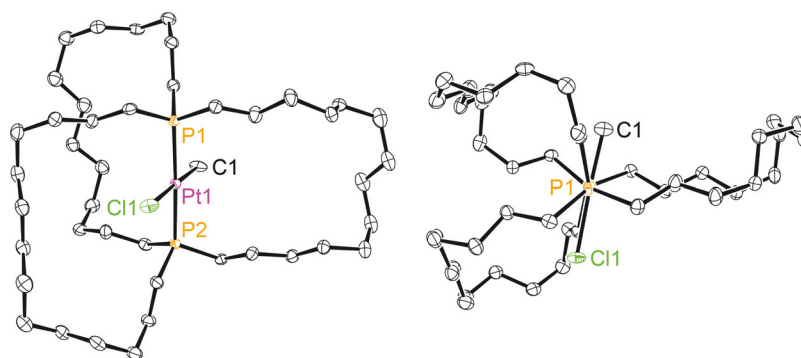
Table 1 Summary of crystallographic data

	<i>cis</i> - 4c	<i>trans</i> - 5c	<i>trans</i> - 7c	<i>trans</i> - 10c
Empirical formula	C ₄₄ H ₉₀ P ₂ Pt	C ₄₃ H ₈₇ ClP ₂ Pt	C ₄₄ H ₈₉ ClP ₂ Pt	C ₄₃ H ₈₇ IP ₂ Pt
Formula weight	876.18	896.60	910.63	988.05
Temperature [K]	110(2)	110(2)	110(2)	110(2)
Diffractometer	Quest	Quest	APEX II	APEX II
Wavelength [Å]	0.71073	0.71073	0.71073	0.71073
Crystal system	Monoclinic	Monoclinic	Monoclinic	Orthorhombic
Space group	<i>P12₁/c1</i>	<i>P12₁/n1</i>	<i>P12₁/c1</i>	<i>Pbca</i>
Unit cell dimensions:				
<i>a</i> [Å]	10.3514(4)	16.2658(9)	38.540(7)	20.481(6)
<i>b</i> [Å]	15.4895(6)	13.6513(8)	14.255(3)	13.685(4)
<i>c</i> [Å]	28.4607(12)	19.9653(11)	25.681(4)	33.232(10)
α [°]	90	90	90	90
β [°]	95.7670(10)	90.909(2)	91.995(2)	90
γ [°]	90	90	90	90
<i>V</i> [Å ³]	4540.2(3)	4432.7(4)	14 100(4)	9314(5)
<i>Z</i>	4	4	12	8
ρ_{calc} [Mg m ⁻³]	1.282	1.344	1.287	1.409
μ [mm ⁻¹]	3.188	3.325	3.137	3.770
<i>F</i> (000)	1848	1880	5736	4048
Crystal size [mm ³]	0.441 × 0.207 × 0.182	0.493 × 0.475 × 0.292	0.10 × 0.10 × 0.10	0.56 × 0.16 × 0.12
θ limit [°]	1.949 to 24.999	1.948 to 27.496	1.66 to 27.50	2.336 to 27.497
Index range (<i>h</i> , <i>k</i> , <i>l</i>)	–12, 12; –18, 18; –33, 33	–21, 21; –17, 17; –25, 25	–50, 50; –18, 18; –33, 33	–26, 26; –17, 17; –43, 43
Reflections collected	102 005	173 120	154 056	97 076
Independent reflections	7997	10 146	32 379	10 629
<i>R</i> (int)	0.0451	0.0537	0.0930	0.0463
Completeness to θ	99.9	99.8	99.9	99.6
Max. and min. transmission	0.4291 and 0.1274	0.2616 and 0.0906	0.7457 and 0.4356	0.7456 and 0.4890
Data/restraints/parameters	7997/801/566	10 146/123/459	32 379/1956/1676	10 629/3/426
Goodness-of-fit on <i>F</i> ²	1.073	1.056	1.056	1.076
<i>R</i> indices (final) [<i>I</i> > 2 σ (<i>I</i>)]				
<i>R</i> ₁	0.0331	0.0183	0.0585	0.0353
<i>wR</i> ₁	0.0695	0.0387	0.1194	0.0837
<i>R</i> indices (all data)				
<i>R</i> ₂	0.0378	0.0226	0.0934	0.0493
<i>wR</i> ₂	0.0732	0.402	0.1364	0.0918
Largest diff. peak and hole [e Å ⁻³]	2.107 and –2.309	0.683 and –0.795	1.927 and –1.925	2.037 and –1.132

Table 2 Key crystallographic bond lengths [Å] and angles [°]

	<i>cis-4c</i>	<i>trans-5c</i> ^a	<i>trans-7c</i> (1) ^b	<i>trans-7c</i> (2) ^b	<i>trans-7c</i> (3) ^b	<i>trans-10c</i> ^a
Pt–P	2.2844(11) 2.2818(11)	2.2810(5) 2.2920(5)	2.2887(16) 2.3089(16)	2.2848(19) 2.3037(19)	2.284(2) 2.285(2)	2.2946(12) 2.3032(13)
Pt–C	2.105(4) 2.106(5)	2.074(7)	2.102(6)	2.093(8)	2.104(8)	2.179(5)
Pt–Cl or I	—	2.4020(6)	2.4052(16)	2.401(2)	2.408(2)	2.6864(8)
P–Pt–P	104.15(4)	176.055(17)	172.37(6)	177.07(7)	172.97(9)	175.55(4)
P–Pt–C	86.76(16) 167.83(15) 87.06(17) 167.78(17)	88.0(3) 90.7(3)	87.77(17) 90.75(17)	88.1(2) 91.6(2)	91.5(2) 87.1(2)	87.66(16) 90.56(16)
C–Pt–C	82.6(2)	—	—	—	—	—
P–Pt–Cl or I	—	92.74(2) 88.70(2)	91.60(6) 90.31(6)	92.29(7) 88.21(7)	90.03(9) 91.85(8)	93.77(3) 88.46(3)
C–Pt–Cl or I	—	177.7(3)	176.6(2)	176.6(3)	176.0(3)	173.42(16)

^a Values for the dominant X–Pt–CH₃ orientation. ^b Values for the three independent molecules in the unit cell.

**Fig. 1** Thermal ellipsoid plots of the molecular structure of *cis-4c* (50% probability level, dominant conformation).**Fig. 2** Thermal ellipsoid plots of the molecular structure of *trans-5c* (50% probability level, dominant conformation).

cis-3c was slurried with the same batch used in Scheme 5. No reaction was observed after 5 h at room temperature or 24 h at 80 °C (entry 4, Table 3). When a mesitylene solution of *cis-3c* was kept at 140 °C for 30 h (entry 3, Table 3), ³¹P{¹H} NMR spectra showed the gradual conversion to two new species, neither of which was *trans-3c* (δ /ppm 7.4 (s, 84%) and 4.3 (s, 16%)).²⁰

When a toluene-*d*₈ solution of the parachute like dimethyl complex *cis-4c* was kept at 80 °C for 10 h (entry 5, Table 3) or slurried at room temperature with silica gel for 24 h (entry 7, Table 3), no reaction was observed. However, when slurried at 80 °C for 24 h (entry 8, Table 3), complete conversion to two unknown species occurred (δ /ppm 11.4 (s, 76%) and 6.2 (s,

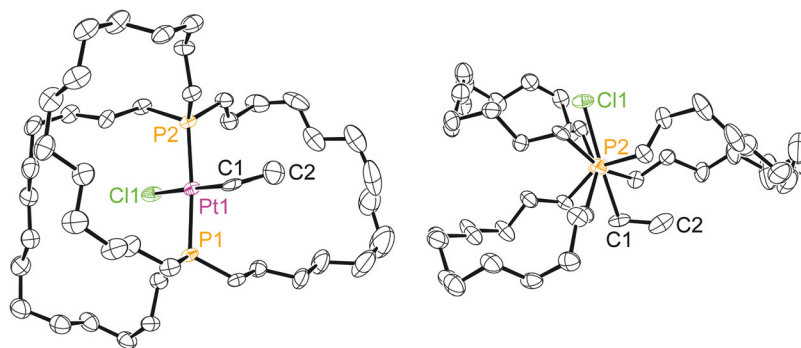


Fig. 3 Thermal ellipsoid plots of the molecular structure of *trans*-7c (50% probability level, one of three independent molecules).

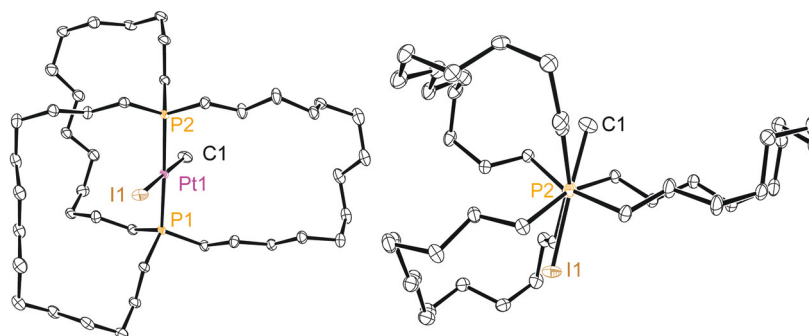


Fig. 4 Thermal ellipsoid plots of the molecular structure of *trans*-10c (50% probability level, dominant conformation).

24%)).²⁰ When a mesitylene solution of *cis*-4c was kept at 140 °C for 30 h, there was *ca.* 16% conversion to an unknown new species.

When a mesitylene solution of the gyroscope like methyl chloride complex *trans*-5c was kept at 140 °C for 30 h (entry 14, Table 3), most of the *trans*-5c remained, with 13% conversion to an unknown species (7.3 ppm; no detectable *cis*-5c). However, an analogous experiment with the corresponding ethyl chloride complex *trans*-7c (entry 15, Table 3) showed the gradual conversion to an unknown product (³¹P{¹H} NMR: 7.4 ppm, s, ¹J_{Pt} = 2447 Hz),²⁰ with one main intermediate (18.3 ppm), the NMR properties of which (Experimental section) indicated a platinum hydride complex (¹H NMR: −16.78 ppm, t, ²J_{HP} = 13.8 Hz).

Next, *o*-C₆H₄Cl₂ solutions of the new parachute like phenyl chloride complex *cis*-8c (Scheme 7) were kept at 100 °C for 6 h or 140 °C for 0.5 h (entries 16 and 17, Table 3). In both cases, >99% conversion to gyroscope like *trans*-8c was observed. Thus, the relative thermodynamic stabilities of the phenyl chloride complexes are analogous to those of the alkyl chloride complexes.

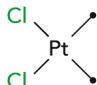
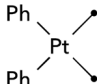
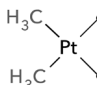
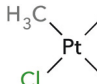
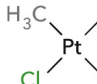
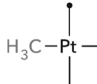
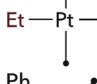
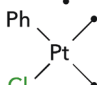
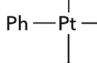
Some attempted thermal equilibrations gave well defined alternative reactions. As shown in Scheme 9, a C₆D₅Br solution of the parachute like dimethyl complex *cis*-4c was kept at 110 °C for 7 h (little change) and then 140 °C for 6 h. The higher temperature gave complete conversion to the gyroscope like methyl bromide complex *trans*-9c, as confirmed by ³¹P and

¹H NMR. Toluene-*d*₅ was also detected. An analogous reaction of the diethyl complex *cis*-6c (140 °C) initially gave what was assigned as the ethyl bromide complex *trans*-Pt(Br)(Et)(P((CH₂)₁₄)₃P) based upon the similar ¹J_{Pt} value (2771 vs. 2806 Hz). With time, this further converted to the previously isolated dibromide complex *trans*-Pt(Br)₂(P((CH₂)₁₄)₃P) (¹J_{Pt} 2347 vs. 2344^{4a} Hz). In another example, an *o*-C₆H₄Cl₂ solution of *cis*-4c was kept at 140 °C for 12 h. Complete conversion to the gyroscope like methyl chloride complex *trans*-5c occurred. In this case, an unknown intermediate could be seen by ³¹P NMR (8.9 ppm, s).

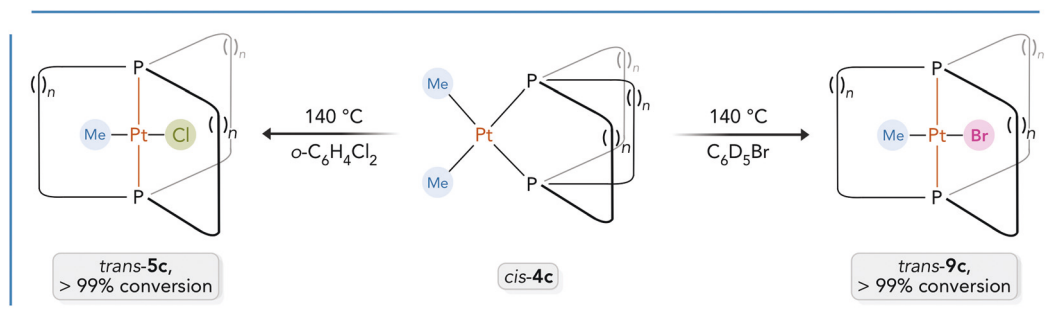
Computational data

In order to better interpret the preceding isomerizations, molecular dynamics simulations followed by DFT optimizations were carried out for all complexes with (CH₂)₁₄ bridges (“c series”) along the lines reported earlier.⁸ The molecular dynamics annealing simulations were run to maximize the likelihood of correctly identifying the lowest energy conformer.²¹ The ten lowest conformations from each trajectory were extracted and “cleaned up” using a semi-empirical method (PM7) followed by DFT optimizations (in the gas phase at 25 °C or 298 K).²² The computed relative energies of these species are shown in Fig. 5. It was critical to incorporate dispersion corrections in order to obtain appropriately folded (CH₂)₁₄ bridges. Subsequently, single point corrections were performed using an implicit solvation model for two typical

Table 3 Summary of thermolysis experiments

Entry	Starting material	Solvent	Temperature (°C)	Time (h)	Result ^a	
1		<i>cis</i> -2c	Toluene- <i>d</i> ₈ or CDCl ₃ /silica gel	25	24	>99 : 1 <i>cis</i> / <i>trans</i> -2c
2		<i>cis</i> -3c	Toluene- <i>d</i> ₈	80	10	>99 : 1 <i>cis</i> / <i>trans</i> -3c
3		Mesitylene	140	30	>99% conv. unknown species ^b	
4		Toluene- <i>d</i> ₈ /silica gel	25, then 80	5, then 24	>99 : 1 <i>cis</i> / <i>trans</i>	
5		Toluene- <i>d</i> ₈	80	10	>99 : 1 <i>cis</i> / <i>trans</i> -4c	
6		Mesitylene	140	30	16% conv. unknown species ^b	
7		Toluene- <i>d</i> ₈ /silica gel	25	24	>99 : 1 <i>cis</i> / <i>trans</i>	
8		Toluene- <i>d</i> ₈ /silica gel	25, then 80	5, then 24	>99% conv. unknown species ^b	
9		<i>cis</i> -5c	Toluene- <i>d</i> ₈ or toluene- <i>d</i> ₀	80	10 or 72	86 : 14 or <1 : >99 <i>cis</i> / <i>trans</i> -5c
10		<i>trans</i> -5c	<i>o</i> -C ₆ H ₄ Cl ₂	100	3	<1 : 99 <i>cis</i> / <i>trans</i> -5c
11		<i>trans</i> -5c	<i>o</i> -C ₆ H ₄ Cl ₂	140	0.5	<1 : 99 <i>cis</i> / <i>trans</i> -5c
12		<i>trans</i> -5c	C ₆ D ₅ Br	110	7	<1 : 99 <i>cis</i> / <i>trans</i> -5c
13		<i>trans</i> -5c	Mesitylene	140	0.5	<1 : 99 <i>cis</i> / <i>trans</i> -5c
14		<i>trans</i> -5c	Mesitylene	140	30	13% conv. unknown species ^b
15		<i>trans</i> -7c	Mesitylene	140	30	>99% conv. unknown species ^{b,c}
16		<i>cis</i> -8c	<i>o</i> -C ₆ H ₄ Cl ₂	100	6	<1 : 99 <i>cis</i> / <i>trans</i> -8c
17		<i>trans</i> -8c	<i>o</i> -C ₆ H ₄ Cl ₂	140	0.5	<1 : 99 <i>cis</i> / <i>trans</i> -8c
18		<i>trans</i> -8c	Mesitylene	140	30	<1 : 99 <i>cis</i> / <i>trans</i> -8c

^a Assayed by ³¹P NMR as detailed in the Experimental section. ^b Chemical shifts are provided in the Experimental section; when only 13–16% conversion is noted, the remaining material is the educt. ^c A platinum hydride intermediate can be observed by ¹H NMR; see text and Experimental section.



Scheme 9 Thermolyses that afford well defined complex/solvent reactions.

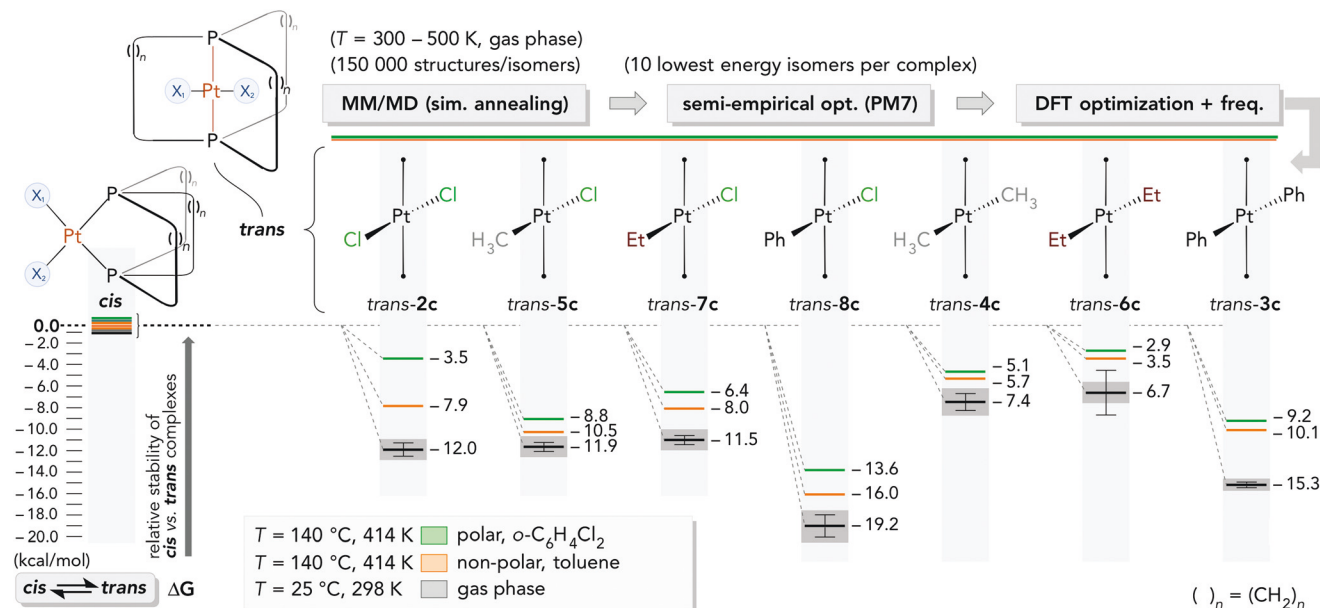


Fig. 5 Relative energies (ΔG , kcal mol⁻¹) of isomeric *cis*/parachute and *trans*/gyroscope platinum complexes as computed by DFT (gas phase or toluene or o -C₆H₄Cl₂ solutions) preceded by molecular dynamics and semi-empirical (PM7) computations.

solvents from Table 3 (o -C₆H₄Cl₂, toluene).²³ Frequency calculations were also performed to confirm that minimum structures were obtained and further to afford temperature corrections to the Gibbs energy at a representative temperature from Table 3 (140 °C or 414 K).

It was also sought to compare the relative energies of acyclic model complexes, which would not be subject to possible ring strain effects derived from the dibridgehead diphosphine ligands. For this purpose, PEt₃ as opposed to PMe₃ was selected for the phosphine ligands, as the former better mimics the electronic effect exerted by the three (CH₂)₁₄ bridges.²⁴ These species are designated with double primes; for example *trans*-2'' represents *trans*-Pt(Cl)₂(PEt₃)₂, the analog of the gyroscope like dichloride complex *trans*-2c.

In Fig. 5 and 6, the energies of the *trans* isomers are displayed relative to those of the *cis* isomers symbolized in the columns at the far left. In Fig. 5, most of the gyroscope isomers are 11.5–19.2 kcal mol⁻¹ more stable than the parachute isomers in the gas phase. However, the energies of the two dialkyl complexes *cis*/*trans*-4c and *cis*/*trans*-6c are closer, with the *trans* isomers 6.7–7.4 kcal mol⁻¹ more stable. Fig. 5 also shows the energy differences for the dichloride complexes *cis*/*trans*-2c. This system was also examined by DFT earlier,⁸ with the important result that the *trans* isomers were more stable for all the (CH₂)_n bridge lengths examined ($n = 10, 12, 14, 16, 18, 20, 22$).¹⁰ All bond lengths and angles about platinum nicely model those determined crystallographically (Table 2 and earlier papers for *trans*-2c,^{4a} *cis*-2c,⁸ *trans*-3c,^{4a} *cis*-3c,⁸ and *trans*-8c^{4b}), and some are depicted in the graphics below.

In Fig. 6, the results for the PEt₃ substituted acyclic model compounds are presented. Here, the gas phase energy differences closely (albeit not perfectly) follow the pattern in Fig. 5,

but average 6.6 kcal mol⁻¹ lower. This suggests that the *cis*/parachute isomers in Fig. 5 are *ca.* 6.6 kcal mol⁻¹ destabilized relative to the *trans*/gyroscope isomers (and/or that the latter are in some manner stabilized). In any case, the *cis* and *trans* dialkyl complexes Pt(R)₂(PEt₃)₂ are rendered approximately equal in energy.

In response to a reviewer inquiry regarding the origin of the 6.6 kcal mol⁻¹ difference, the PtX₂ or PtXX' fragments were excised from the structures of all *cis*/parachute and *trans*/gyroscope complexes in Fig. 5, in each case taking the most favorable of the ten conformations analyzed. Single point calculations were carried out on the remaining dibridgehead diphosphines, a process that freezes the phosphorus–phosphorus distances (3.4–3.5 vs. 4.5–4.6 Å) and all other atoms. In all cases, the gas phase energies of the gyroscope derived diphosphines were lower (2.8–7.3 kcal mol⁻¹). Next, the diprimary and dissecondary diphosphines H₂P(CH₂)₁₄PH₂ and HP((CH₂)₁₄)₂PH, derived by deleting two and one (CH₂)₁₄ bridges, respectively, were similarly examined. A detailed analysis of the results (see highlights in the ESI†) suggests that bridge/bridge interactions provide stabilization in the *trans*/gyroscope systems. Torsional interactions and angle strain (*e.g.*, at phosphorus) seemingly have subordinate roles in the energy differences. Further analysis is provided below and in the ESI.†

Discussion

Preliminary remarks

Schemes 3–8 diagram a number of substitution reactions involving gyroscope and parachute like complexes. Although this study is concerned with general isomerization rates and

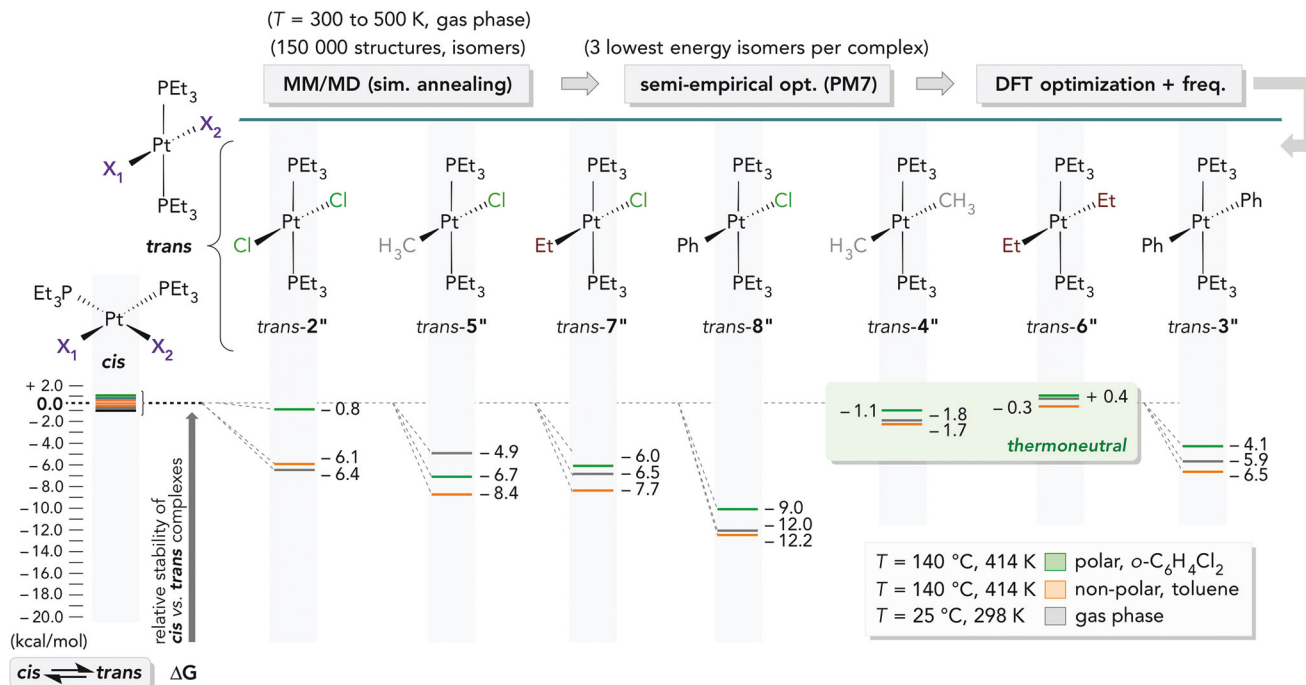
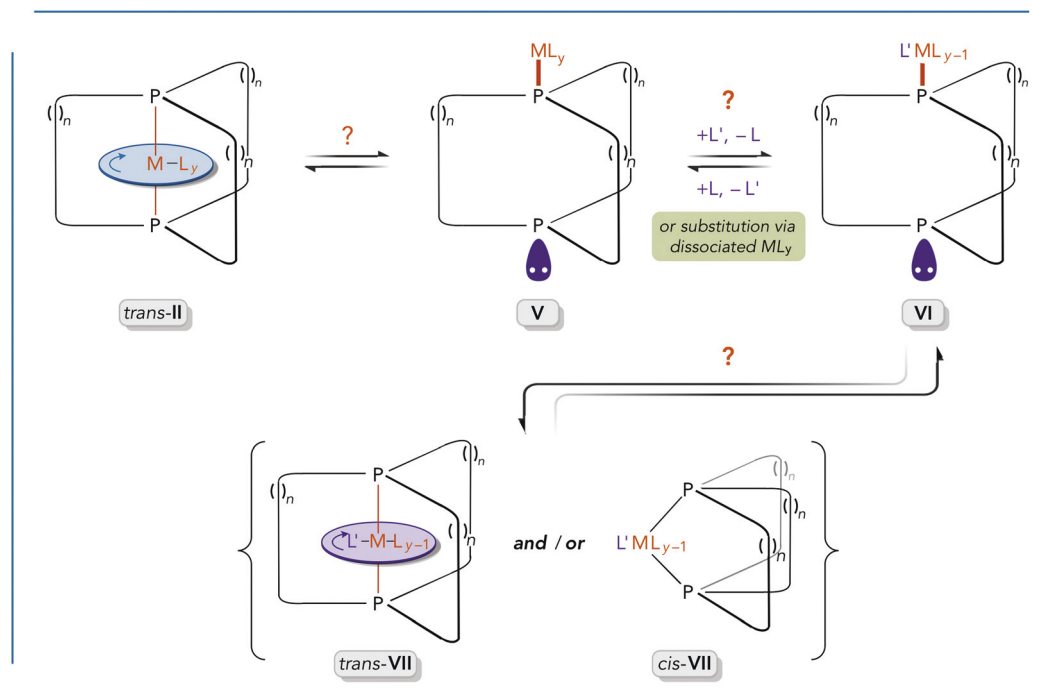


Fig. 6 Relative energies (ΔG , kcal mol^{-1}) of isomeric *cis* and *trans* platinum complexes with acyclic triethylphosphine ligands as computed by DFT (gas phase or toluene or $o\text{-C}_6\text{H}_4\text{Cl}_2$ solutions) preceded by molecular dynamics and semi-empirical (PM7) computations.

equilibria as opposed to mechanism, it should be noted that substitution mechanisms of square planar platinum(II) complexes have been extensively studied, going back more than 60 years.^{25,26} However, the gyroscope like complexes may have

pathways available that lack counterparts in classical complexes. For example, equilibria exist that allow the ML_y rotators to “escape” from their cages.^{4a,5c,27,28} A possible initial step is shown in Scheme 10 ($\text{trans-II} \rightarrow \text{V}$). This entails the cleavage of



Scheme 10 Potential equilibria that may play a role in substitution reactions.

one metal–phosphorus bond and isomerization of the dibridgehead diphosphine ligand from an “in/in” to an “out/out” geometry.²⁹ Such isomerizations are facile with the free diphosphines.²⁸

Thus, there exists the possibility that substitution occurs external to the cage, perhaps involving **V** directly, or another transient species. Furthermore, as shown in Scheme 10, either gyroscope (*trans*-**VII**) or parachute (*cis*-**VII**) products could be preferred kinetically. Also, per studies of related acyclic platinum(II) complexes, mechanisms would be expected to differ depending upon the attacking group, especially for nucleophilic or organometallic agents such as RLi *versus* electrophilic agents such as HCl.¹⁷ Finally, although purely thermal *cis/trans* isomerizations of platinum(II) complexes have been established, a wide variety of catalysts have been documented.^{11,30–32} To sum, this digression conveys the diversity of phenomena that might play roles in Schemes 3–8, but are beyond the scope of the present investigation.

Coordination geometries: *trans*/gyroscope *versus cis*/parachute

One starting point for analysis involves the gyroscope and parachute like dichloride complexes *trans*-**2** and *cis*-**2** (Scheme 2). As reported earlier,⁸ both DFT and thermolysis data (Scheme 2) show the former to be more stable, at least for (CH₂)_n bridges with *n* ≥ 10. In syntheses where the educts cannot bias the stereochemical outcome – for example,²⁷ PtCl₂ and the dibridgehead diphosphine P((CH₂)₁₄)₃P – *trans*-**2** is always the exclusive product. The new computational data in Fig. 5 and 6 establish an intrinsic energetic preference for the gyroscope like isomers (*ca.* 6.6 kcal mol^{−1} with (CH₂)₁₄ bridges). The single point calculations with P((CH₂)₁₄)₃P localize the principal origin of the energy differences within the diphosphine ligands. The additional calculations with HP((CH₂)₁₄)₂PH and H₂P((CH₂)₁₄)PH₂ point to non-covalent chain/chain interactions, and any attendant dispersion forces, as stabilizing factors in the gyroscope systems. Efforts to identify destabilizing steric features unique to the parachute systems have so far not been successful.

Computations have previously been carried out with related phosphite complexes, for which only parachute like *cis* isomers have been synthetically accessed.⁸ Here the DFT data show the *cis* isomers to be considerably more stable. Since phosphite ligands are stronger π acceptors than phosphine ligands,^{33,34} geometries in which the π donor chloride ligands³⁵ are *trans* to the phosphorus donor atoms become preferred. In other words, this favorable electronic interaction dominates over any steric factors that may prefer gyroscope like dibridgehead diphosphite complexes.

Alkyl ligands are considered to be strong σ donors – indeed, the strongest among the ligands in this study³⁴ – and in the context of the *trans* influence (*vide infra*), *trans* geometries are considered to be particularly unfavorable. From this perspective, the formation of the parachute like dialkyl complexes *cis*-**4c,e,g** and *cis*-**6c** in Schemes 4 and 6 is less surprising. However, we were unable to access any of the corresponding *trans* isomers, precluding an experimental confirmation of the

relative stabilities. Thus, two scenarios remain in play: (a) *cis*-**4c,e,g** and *cis*-**6c** represent kinetically but not thermodynamically favored substitution products and conditions for isomerizations to *trans*-**4c,e,g** and *trans*-**6c** remain to be developed, or (b) *cis*-**4c,e,g** and *cis*-**6c** represent thermodynamically favored substitution products, either produced directly (kinetic products) or *via* transient *trans* isomers.

In our opinion, the computational data fit best with the latter. Although parachute like *cis*-**4c** and *cis*-**6c** remain 7.4–6.7 kcal mol^{−1} less stable than gyroscope like *trans*-**4c** and *trans*-**6c** in the gas phase (Fig. 5), these differences narrow to 5.7–2.9 kcal mol^{−1} in toluene or *o*-C₆H₄Cl₂, with the diminution always more pronounced in the more polar dichlorinated solvent. For the acyclic model compounds **4**” and **6**” (Fig. 6), the *cis* and *trans* isomers have essentially equal energies. In addition, ethyl is a stronger σ donor than methyl,³⁶ further destabilizing the *trans* isomers. In any case, Fig. 5 reproduces the relative trends in our data, although *trans*-**4c** and *trans*-**6c** appear overstabilized compared to their *cis* isomers.³⁷

Consider next the diphenyl complexes **3** introduced in Scheme 3. The computations in Fig. 5 indicate much greater stabilities for the *trans*/gyroscope *versus cis*/parachute isomers as compared to the dialkyl analogs. The same trend is seen with the acyclic analogs in Fig. 6. The ligating sp² carbon atom of a phenyl ligand constitutes a weaker σ donor than the sp³ carbon atom of an alkyl ligand,³⁶ attenuating the electronic mismatch in the *trans* isomers.³⁸ However, numerous experimental attempts to establish equilibria (Table 3) have been unsuccessful. Regardless, it can be concluded that the reaction of *cis*-**2c** and Ph₂Zn to give *cis*-**3c** (Scheme 3) is under kinetic control.

The remaining equilibrium issues in Schemes 3–8 are quite clear cut. In all cases, it can be shown experimentally that the *trans*/gyroscope methyl or phenyl chloride complexes **5c,e,g** and **8c** are much more stable than the *cis*/parachute analogs (Schemes 5 and 7), and the same can be presumed for the ethyl chloride complex **7c** (Scheme 6). These trends are fully supported by the computations. In all cases the weak σ donor chloride ligand is preferentially directed opposite to the stronger alkyl or phenyl σ donor.³⁴

There still remain various open questions. For example, a reviewer inquired regarding the mechanism of the *cis/trans* isomerizations that take place over silica gel in Scheme 5. Silica gel promotes or catalyzes quite a broad spectrum of organic reactions,³⁹ but to the authors’ knowledge has not been previously observed to effect geometric isomerizations of metal complexes. Nonetheless, given the plethora of *cis/trans* equilibration mechanisms established for square planar platinum(II) complexes,^{11,30–32} many possible roles are easily envisioned. Since isomerization also occurs upon attempted Et₂O/ROH crystallization, perhaps the hydroxyl groups associated with silica are involved.

Further electronic and structural considerations

The preceding analysis made little reference to the “*trans* influence”, which is considered the thermodynamic counterpart of

the “*trans* effect”.^{25,26,40,41} There have been extensive studies of these phenomena in platinum(II) chemistry. For the ligands of interest in this paper, the *trans* influence increases in the order $\text{Cl}^- < \text{I}^- < \text{Ph}^- < \text{PR}_3 < \text{Me}^- < \text{Et}^-$.^{36,41c} However, these concepts are often applied rather simplistically, although even in early studies it was appreciated that the trends represent a complex mash-up of σ and π donor/acceptor effects, the relative importance of which can vary from substrate to substrate.⁴² Accordingly, correlations with the equilibria established above are not attempted.

Much work involving the *trans* influence has been focused upon structural trends – specifically, the effect of a series of *trans* ligands upon a metal–ligand bond distance. A longer bond *trans* to the ligand of interest is taken as evidence of destabilization, and a shorter bond is taken as evidence for stabilization.^{36,40,41} One question is whether our computed structures, excerpted in Fig. 7, conform to these expectations.

For example, with the chloride substituted gyroscope like complexes *trans*-7c, *trans*-5c, *trans*-8c, and *trans*-2c, the platinum–chlorine bond lengths (2.47, 2.46, 2.44, 2.35 Å) contract as the *trans* influences of the ethyl, methyl, phenyl, and chloride ligands decrease. The same trend holds for the platinum–carbon bond lengths in the diethyl, dimethyl, and diphenyl complexes *trans*-6c, *trans*-4c, and *trans*-3c (2.16, 2.15, 2.09 Å). With the *cis*/parachute complexes, the platinum–phosphorus bond lengths do not change as much as the *trans* ligand is varied, except in the case of the dichloride complex *cis*-2c (2.28 Å vs. 2.38–2.39 Å for *trans* ethyl, methyl, and phenyl ligands). However, the platinum–carbon bond lengths follow the same trends as in the *trans* complexes. They are (as compared to *trans* complexes) uniformly longer in *cis*-5c, *cis*-7c, and *cis*-8c (all bonds *cis* to chloride), and shorter in *cis*-4c, *cis*-6c, and *cis*-3c (all bonds *cis* to alkyl).

The experimental structural data for *cis*-4c, *trans*-5c, and *trans*-7c (Table 2) are in excellent agreement with the bond lengths in Fig. 7 and other computed metrical parameters. All values are in the normal ranges for square planar platinum(II) complexes.^{43–45} The analogous methyl and ethyl chloride complexes *trans*-5c and *trans*-7c exhibit bond lengths and angles about platinum that are within experimental error. In the

methyl chloride and iodide complexes *trans*-5c and *trans*-10c, the platinum–carbon bonds lengthen from 2.074(7) Å to 2.179(5) Å. This can be attributed to the greater *trans* influence of the iodide ligand noted above.^{25,41c}

Additional properties of new complexes

Although this study is not concerned with the dynamic properties of the complexes in Schemes 3–8, certain features are apparent from the ¹³C NMR spectra. Specifically, all of the *trans*/gyroscope complexes in the “c series” exhibit only seven signals. This indicates that rapid ML_y rotation (or $(\text{CH}_2)_{14}$ bridge exchange) takes place on the NMR time scale at room temperature (with the number of signals, 14/2, reflecting the formal horizontal mirror plane). Similar behavior has been observed with other methyl substituted rotors,^{5c,7} but *trans*-7c represents the first case with a larger ethyl ligand. The analogs with longer $(\text{CH}_2)_n$ bridges, *trans*-4e,g, also gave the minimum number of ¹³C NMR signals. These processes have been analyzed in depth in a recent review that collects all available activation parameters.³ A key consideration involves the van der Waals radii of the ML_y rotators *versus* the clearance allowed by the $(\text{CH}_2)_n$ bridges.

In contrast, the parachute like complex *cis*-3c exhibits eleven CH_2 ¹³C NMR signals, indicating that the “jump rope” process is slow on the NMR time scale at room temperature. In theory, two sets of seven signals with a *ca.* 2 : 1 intensity ratio should be observable, but sufficient resolution was not available at 126 MHz. As reported earlier, the corresponding dichloride complex *cis*-2c exhibits twelve signals.⁸ The higher homologs *cis*-3e,g give the minimum number of signals (nine and eleven), indicative of rapid jump rope processes.

The thermolyses in Scheme 9 convert the parachute like dimethyl complex *cis*-4c to the gyroscope like methyl halide complexes *trans*-5c and *trans*-9c. This suggests an initial oxidative addition of the high boiling haloarene solvent to give a platinum(IV) species, a type of reaction with significant precedent.⁴⁶ Indeed, toluene-*d*₅ can be identified as a product in the reaction with bromobenzene-*d*₅. Evidence has also been obtained from related reactions for the formation of species with new platinum–carbon bonds. Another fascinating lead

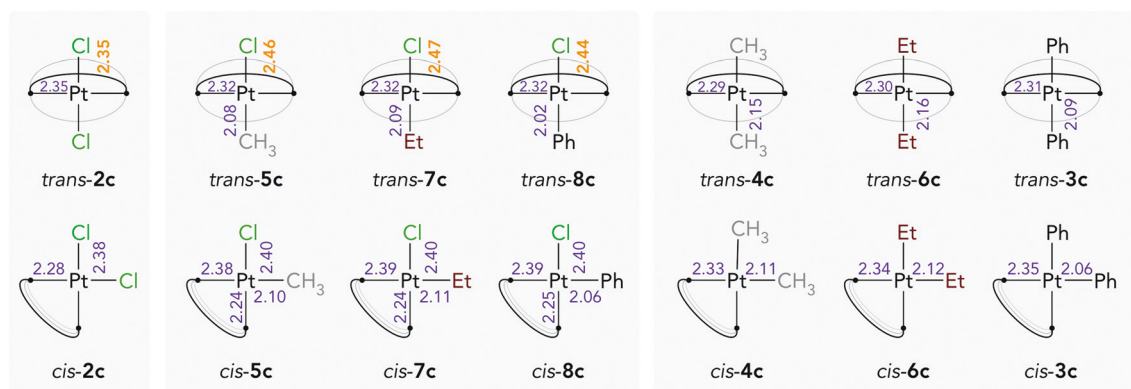


Fig. 7 Platinum–ligand bond lengths (Å) for computed *trans*/gyroscope and *cis*/parachute complexes.

only briefly mentioned above is the apparent formation of a platinum bis(phosphine) hydride intermediate upon attempted isomerization of the ethyl chloride complex *trans*-5c. All of these transformations and the mesitylene-derived products in Table 3 remain under active investigation.

Summary

With respect to the gyroscope like dichloride complexes *trans*-2c,e,g, this study has established that isomerization normally accompanies reactions with alkyl lithium reagents to give the dialkyl complexes *cis*-4c,e,g and *cis*-6c (Schemes 4 and 6). In contrast, phenyl nucleophiles normally afford *trans* diphenyl complexes, although lesser amounts of *cis* adducts are sometimes observed in reactions with PhLi. Subsequent reactions of *cis*-4c,e,g and HCl (1.0 equiv.) give detectable quantities of *cis* alkyl chloride complexes that easily convert (over silica gel or at ~100 °C) to the gyroscope like isomers *trans*-5c,e,g. The *cis* phenyl chloride complex *cis*-8c undergoes an analogous thermal isomerization to *trans*-8c. DFT calculations indicate that the *trans*/gyroscope complexes always have lower energies than the *cis*/parachute complexes in the gas phase. However, isomeric dimethyl and diethyl complexes have nearly the same energies in *o*-C₆H₄Cl₂.³⁷ With acyclic model compounds the energy differences are much less, and the isomeric dimethyl and diethyl complexes exhibit essentially equal energies.

Overall, this work has brought several concepts from traditional platinum(II) coordination chemistry into the modern context of the chelating and potentially *trans* spanning dibridgehead diphosphine ligands P((CH₂)_n)₃P. These data greatly enhance the confidence with which the NMR data associated with various dynamic processes can be interpreted. These include ML₂ rotation in the gyroscope like complexes and the “jump rope” (CH₂)_n exchange in the parachute like complexes, both of which will be topics of future reports.

Experimental section

General

Reactions were conducted under nitrogen atmospheres unless noted. Materials were utilized as follows: Et₂O, CH₂Cl₂, and THF, purified by a Glass Contour system; hexanes (98.5%, Sigma-Aldrich), EtOAc (99.5%, Sigma-Aldrich), methanol (99.8%, Sigma-Aldrich), benzene (99.88%, Sigma-Aldrich), mesitylene (97%, TCI), *o*-C₆H₄Cl₂ (99%, Sigma-Aldrich), CDCl₃, C₆D₆, toluene-*d*₈, C₆D₅Br (4 × Cambridge Isotopes), MeLi (1.6 M in Et₂O, Sigma-Aldrich), EtLi (0.50 M in benzene, Sigma-Aldrich), PhLi (1.8 M in Bu₂O, Sigma-Aldrich), CH₃COCl (98%, Alfa-Aesar), HCl (2.0 M in Et₂O, Alfa-Aesar), Et₃N (99%, Alfa-Aesar), LiBr (99.99%, Alfa-Aesar), NaI (99%, EMD), celite (EMD), silica gel (40–63 μm, 230–400 mesh, Silicycle), and neutral alumina (Brockmann I, for chromatography, 40–300 μm, 60A, Acros), used as received.

NMR spectra were recorded on standard 500 MHz FT spectrometers at ambient probe temperatures and referenced as follows (δ, ppm): ¹H: residual internal CHCl₃ (7.26) or C₆D₅H

(7.16); ¹³C{¹H}: internal CDCl₃ (77.16) or C₆D₆ (128.06); ³¹P{¹H}: external 85% H₃PO₄ (0.00). Melting points were determined on a Stanford Research Systems (SRS) MPA100 (Opti-Melt) automated device. Microanalyses were conducted by Atlantic Microlab.

***cis*-Pt(Me)₂(P((CH₂)₁₄)₃P) (*cis*-4c).** A Schlenk flask was charged with *trans*-Pt(Cl)₂(P((CH₂)₁₄)₃P) (*trans*-2c;^{4a} 0.2242 g, 0.2445 mmol) and Et₂O (12 mL). Then MeLi (1.6 M in Et₂O, 0.330 mL, 0.528 mmol) was added with stirring (rt). After 12 h, the mixture was exposed to air. After 1 h, the sample was filtered through celite, which was washed with Et₂O (10–20 mL). The solvent was removed from the filtrate by rotary evaporation. The residue was chromatographed on neutral alumina (1 : 0.005 v/v hexanes/Et₃N). The solvent was removed from the product containing fractions (TLC monitoring) by rotary evaporation. The oil was kept at 4 °C, and after 2 d gave *cis*-4c as a white solid (0.1645 g, 0.1877 mmol, 77%), mp (open capillary) 80–83 °C. Anal. Calcd for C₄₄H₉₀P₂Pt (876.21): C, 60.31; H, 10.35. Found: C, 60.59; H, 10.55. MS (MALDI-TOF, *m/z*, relative intensity): 875.6 ([M]⁺, 19%), 860.6 ([M – CH₃]⁺, 100%).

NMR (CDCl₃, δ/ppm):⁴⁷ ¹H (500 MHz) 1.90–1.78 (br m, 4H, PCH₂), 1.72–1.50 (br m, 12H, CH₂), 1.50–1.21 (br m, 68H, remaining CH₂), 0.30 (dd, 6H, ³J_{HP(trans)} = 7.1 Hz, ³J_{HP(cis)} = 6.1 Hz, ²J_{HPT} = 66 Hz,⁴⁸ PtCH₃); ¹³C{¹H} (126 MHz) 31.1 (virtual t,⁴⁹ J_{CP} = 4.2 Hz, PCH₂CH₂CH₂), 30.5 (virtual t,⁴⁹ J_{CP} = 6.6 Hz, PCH₂CH₂CH₂), 28.3 (s, CH₂), 27.52 (s, CH₂), 27.46 (s, CH₂), 27.2 (s, CH₂), 26.9 (s, CH₂), 26.5 (s, CH₂), 26.4 (s, CH₂), 24.8 (virtual t,⁴⁹ J_{CP} = 10.5 Hz, PCH₂CH₂), 23.3 (apparent br m, PCH₂), 2.8 (dd, ²J_{CP(trans)} = 101.7 Hz, ²J_{CP(cis)} = 9.9 Hz, PtCH₃); ³¹P{¹H} (202 MHz) 6.9 (s, ¹J_{PPT} = 1886 Hz).⁴⁸

***cis*-Pt(Me)₂(P((CH₂)₁₈)₃P) (*cis*-4e).** A. A Schlenk flask was charged with *trans*-Pt(Cl)₂(P((CH₂)₁₈)₃P) (*trans*-2e;^{4a} 0.1239 g, 0.1142 mmol) and Et₂O (20 mL). Then MeLi (1.6 M in Et₂O, 0.160 mL, 0.256 mmol) was added with stirring (rt). After 12 h, the mixture was exposed to air. After 1 h, the sample was filtered through celite, which was washed with diethyl ether (10–20 mL). The solvent was removed from the filtrate by rotary evaporation. The residue was chromatographed on neutral alumina (1 : 0.005 v/v hexanes/Et₃N). The solvent was removed from the product containing fractions (TLC monitoring) by rotary evaporation to give *cis*-4e as a colorless oil (0.0838 g, 0.0802 mmol, 70%). B. A Schlenk flask was charged with *trans*-2e (0.1436 g, 0.1323 mmol) and Et₂O (25 mL). Then MeLi (1.6 M in Et₂O, 0.210 mL, 0.336 mmol) was added with stirring (rt). After 12 h, the mixture was exposed to air. After 1 h, the sample was filtered through celite, which was washed with Et₂O (10–20 mL). The solvent was removed from the filtrate by rotary evaporation to give *cis*-4e as a beige oil (0.1298 g, 0.1243 mmol, 94%), which solidified after 4 d, mp (open capillary) 48–51 °C. Anal. Calcd for C₅₆H₁₁₄P₂Pt (1044.53): C, 64.39; H, 11.00. Found: C, 64.69; H, 11.19.

NMR (CDCl₃, δ/ppm):⁴⁷ ¹H (500 MHz) 1.77–1.64 (br m, 12H, PCH₂), 1.48–1.39 (br m, 12H, PCH₂CH₂), 1.39–1.33 (br m, 12H, PCH₂CH₂CH₂), 1.33–1.18 (br m, 72H, remaining CH₂), 0.33 (dd, 6H, ³J_{HP(trans)} = 6.7 Hz, ³J_{HP(cis)} = 5.7 Hz, ²J_{HPT} = 65 Hz,⁴⁸

PtCH_3); $^{13}\text{C}\{^1\text{H}\}$ (126 MHz) 31.5 (virtual t, $^{49}J_{\text{CP}} = 5.9$ Hz, $\text{PCH}_2\text{CH}_2\text{CH}_2$), 29.3 (s, CH_2), 29.0 (s, CH_2), 28.5 (s, CH_2), 27.9 (s, CH_2), 27.6 (s, CH_2), 27.2 (s, CH_2), 24.74 (apparent br m, PCH_2CH_2), 24.67 (s, PCH_2), 2.6 (dd, $^2J_{\text{CP}(\text{trans})} = 101.1$ Hz, $^2J_{\text{CP}(\text{cis})} = 10.0$ Hz, PtCH_3); $^{31}\text{P}\{^1\text{H}\}$ (202 MHz) 4.5 (s, $^1J_{\text{PPT}} = 1860$ Hz).⁴⁸

cis-Pt(Me)₂(P((CH₂)₂₂)₃P) (cis-4g). A Schlenk flask was charged with *trans*-Pt(Cl)₂(P((CH₂)₂₂)₃P) (*trans*-2g;^{4c} 0.1469 g, 0.1172 mmol) and Et₂O (20 mL). Then MeLi (1.6 M in Et₂O, 0.170 mL, 0.272 mmol) was added with stirring (rt). After 12 h, the mixture was exposed to air. After 1 h, the sample was filtered through celite, which was washed with Et₂O (10–20 mL). The solvent was removed from the filtrate by rotary evaporation. The residue was dissolved in benzene and sample freeze dried to give *cis*-4g as a white powder (0.1294 g, 0.1067 mmol, 91%), mp (open capillary) 55–60 °C. Anal. Calcd for C₆₈H₁₃₈P₂Pt (1212.84): C, 67.34; H, 11.47. Found: C, 67.61; H, 11.64.

NMR (C₆D₆, δ/ppm):⁴⁷ ^1H (500 MHz) 1.90–1.79 (br m, 12H, PCH_2), 1.70–1.58 (br m, 12H, PCH_2CH_2), 1.49–1.42 (br m, 12H, $\text{PCH}_2\text{CH}_2\text{CH}_2$) 1.42–1.32 (br m, 96H, remaining CH_2), 1.08 (dd, 6H, $^3J_{\text{HP}(\text{trans})} = 7.3$ Hz, $^3J_{\text{HP}(\text{cis})} = 6.1$ Hz, $^2J_{\text{HPt}} = 66$ Hz,⁴⁸ PtCH_3); $^{13}\text{C}\{^1\text{H}\}$ (126 MHz) 32.0 (virtual t, $^{49}J_{\text{CP}} = 5.8$ Hz, $\text{PCH}_2\text{CH}_2\text{CH}_2$), 29.98 (s, CH_2), 29.97 (s, CH_2), 29.85 (s, CH_2), 29.5 (s, CH_2), 29.0 (s, CH_2), 28.5 (s, CH_2), 28.2 (s, CH_2), 27.9 (s, CH_2), 25.4 (apparent br m, PCH_2CH_2), 25.2 (virtual t, $^{49}J_{\text{CP}} = 9.3$ Hz, PCH_2), 3.9 (dd, $^2J_{\text{CP}(\text{trans})} = 101.7$ Hz, $^2J_{\text{CP}(\text{cis})} = 10.0$ Hz, PtCH_3); $^{31}\text{P}\{^1\text{H}\}$ (202 MHz) 4.6 (s, $^1J_{\text{PPT}} = 1853$ Hz).⁴⁸

cis-Pt(Cl)(Me)(P((CH₂)₁₄)₃P) (cis-5c). Under air, a round bottom flask was charged with *cis*-3c (0.4007 g, 0.4573 mmol), CH₂Cl₂ (10 mL), and methanol (1.0 mL). Then CH₃COCl (0.0344 mL, 0.4865 mmol) was added with stirring. After 0.5 h, the solvent was removed by rotary evaporation. The white solid was chromatographed on neutral alumina (25 : 1 : 0.2 v/v/v hexanes/EtOAc/Et₃N). The solvent was removed from the product containing fractions (TLC monitoring) by rotary evaporation to give *cis*-5c as a white solid (0.3610 g, 0.4026 mmol, 83%), mp (open capillary) 122–127 °C. Anal. Calcd for C₄₃H₈₇ClP₂Pt (896.63): C, 57.60; H, 9.78. Found: C, 57.80; H, 10.00.

NMR (CDCl₃, δ/ppm):⁴⁷ ^1H (500 MHz) 2.42–2.33 (br m, 2H, PCH_2), 1.92–1.83 (br m, 2H, CH_2), 1.82–1.68 (br m, 6H, CH_2), 1.68–1.53 (br m, 6H, CH_2), 1.50–1.21 (br m, 68H, remaining CH_2), 0.58 (dd, 3H, $^3J_{\text{HP}(\text{trans})} = 7.0$ Hz, $^3J_{\text{HP}(\text{cis})} = 4.0$ Hz, $^2J_{\text{HPt}} = 50$ Hz,⁴⁸ PtCH_3); $^{13}\text{C}\{^1\text{H}\}$ (126 MHz) 30.9 (virtual t, $^{49}J_{\text{CP}} = 10.5$ Hz, $\text{PCH}_2\text{CH}_2\text{CH}_2$), 30.6 (s, CH_2), 30.5 (s, CH_2), 30.4 (s, CH_2), 30.2 (s, CH_2), 28.5 (s, CH_2), 28.3 (s, CH_2), 27.7 (s, CH_2), 27.4 (s, CH_2), 27.29 (s, CH_2), 27.26 (s, CH_2), 27.1 (s, CH_2), 27.0 (s, CH_2), 26.94 (s, CH_2), 26.90 (s, CH_2), 26.88 (s, CH_2), 26.8 (s, CH_2), 26.33 (s, CH_2), 26.26 (s, CH_2), 26.2 (s, CH_2), 25.0 (s, CH_2), 24.96 (s, CH_2), 24.93 (s, CH_2), 23.9 (s, CH_2), 23.6 (s, CH_2), 23.5 (s, CH_2), 22.8 (virtual t, $^{49}J_{\text{CP}} = 7.3$ Hz, PCH_2), 4.5 (dd, $^2J_{\text{CP}(\text{trans})} = 93.1$ Hz, $^2J_{\text{CP}(\text{cis})} = 8.0$ Hz, PtCH_3); $^{31}\text{P}\{^1\text{H}\}$ (202 MHz) 11.6 (d, $^2J_{\text{PP}} = 12.1$ Hz, $^1J_{\text{PPT}} = 1765$ Hz,⁴⁸ *trans* to CH₃), 5.0 (d, $^2J_{\text{PP}} = 12.1$ Hz, $^1J_{\text{PPT}} = 4278$ Hz,⁴⁸ *cis* to CH₃).

trans-Pt(Cl)(Me)(P((CH₂)₁₄)₃P) (trans-5c). A. Under air, a round bottom flask was charged with *cis*-4c (0.0245 g,

0.0273 mmol), silica gel (0.2577 g), and CH₂Cl₂ (2.5 mL). The mixture was stirred (rt). After 12 h, the sample was filtered and the silica gel further washed with CH₂Cl₂ (25 mL). The solvent was removed from the filtrate by rotary evaporation to yield a colorless oil, which solidified after 4 h to give *trans*-5c (0.0174 g, 0.0192 mmol, 70%) as a white solid, mp (open capillary) 123–127 °C. Anal. Calcd for C₄₃H₈₇ClP₂Pt (896.63): C, 57.60; H, 9.78. Found: C, 57.85; H, 10.05. B. Under air, a vial was charged with *cis*-5c (0.0255 g, 0.0284 mmol), silica gel (0.9528 g) and CH₂Cl₂ (10.0 mL). The mixture was stirred (rt). After 12 h, the sample was filtered and the silica gel further washed with CH₂Cl₂ (50 mL). The solvent was removed from the filtrate by rotary evaporation to yield a colorless oil, which solidified after 1 d to give *trans*-5c (0.0227 g, 0.0253 mmol, 89%) as a white solid. C. As described in the Crystallography section below, *trans*-5c was also obtained upon attempted crystallization of *cis*-5c.

NMR (CDCl₃, δ/ppm):⁴⁷ ^1H (500 MHz) 1.85–1.73 (br m, 12H, PCH_2), 1.65–1.55 (br m, 12H, PCH_2CH_2), 1.48–1.38 (br m, 12H, $\text{PCH}_2\text{CH}_2\text{CH}_2$), 1.38–1.23 (br m, 48H, remaining CH_2), 0.31 (t, 3H, $^3J_{\text{HP}} = 6.2$ Hz, $^2J_{\text{HPt}} = 83$ Hz,⁴⁸ PtCH_3); $^{13}\text{C}\{^1\text{H}\}$ (126 MHz) 30.2 (virtual t, $^{49}J_{\text{CP}} = 6.7$ Hz, $\text{PCH}_2\text{CH}_2\text{CH}_2$), 28.3 (s, CH_2), 27.4 (s, CH_2), 27.3 (s, CH_2), 27.0 (s, CH_2), 23.5 (br s, PCH_2CH_2), 22.0 (virtual t, $^{49}J_{\text{CP}} = 15.7$ Hz, PCH_2), –23.6 (t, $J_{\text{CP}} = 6.4$ Hz, PtCH_3); $^{31}\text{P}\{^1\text{H}\}$ (202 MHz) 10.8 (s, $^1J_{\text{PPT}} = 2824$ Hz).⁴⁸

cis-Pt(Cl)(Me)(P((CH₂)₁₈)₃P) (cis-5e) and trans-5e. A. Under air, a round bottom flask was charged with *cis*-4e (0.0838 g, 0.0802 mmol), CH₂Cl₂ (8 mL), and methanol (0.4 mL). Then HCl (2.0 M in Et₂O, 0.040 mL, 0.080 mmol) was added with stirring. After 0.5 h, the solvent was removed by rotary evaporation. The white solid was chromatographed on neutral alumina (first 3 : 1 : 0.02 v/v/v hexanes/CH₂Cl₂/Et₃N, then 25 : 1 : 0.2 v/v/v hexanes/EtOAc/Et₃N). The solvent was removed from the product containing fractions (TLC monitoring) by rotary evaporation. This gave *trans*-5e (0.0389 g, 0.0365 mmol, 46%), with subsequent fractions affording *trans*-5e/*cis*-5e mixtures. B. A vial was charged with a *trans*-5e/*cis*-5e mixture (0.0274 g, 0.0257 mmol; obtained from a different run of procedure A, ca. 1 : 2 by ^{31}P NMR), silica gel (1.2375 g) and CH₂Cl₂ (10 mL). The mixture was stirred (rt). After 12 h, the sample was filtered and the silica gel further washed with CH₂Cl₂ (40 mL). The solvent was removed from the filtrate to give *trans*-5e (0.0165 g, 0.0155 mmol, 60%) as a beige oil.

Data for cis-5e: NMR (CDCl₃, δ/ppm): $^{31}\text{P}\{^1\text{H}\}$ (202 MHz) 10.3 (d, $^2J_{\text{PP}} = 12.3$ Hz, $^1J_{\text{PPT}} = 1750$ Hz, *trans* to CH₃), 3.56 (d, $^2J_{\text{PP}} = 12.1$ Hz, $^1J_{\text{PPT}} = 4362$ Hz, *cis* to CH₃).

Data for trans-5e: NMR (CDCl₃, δ/ppm):⁴⁷ ^1H (500 MHz) 1.88–1.75 (br m, 12H, PCH_2), 1.65–1.50 (br m, 12H, PCH_2CH_2), 1.46–1.38 (br m, 12H, $\text{PCH}_2\text{CH}_2\text{CH}_2$), 1.38–1.23 (br m, 72H, remaining CH_2), 0.31 (t, 3H, $^3J_{\text{HP}} = 6.2$ Hz, $^2J_{\text{HPt}} = 83$ Hz,⁴⁸ PtCH_3); $^{13}\text{C}\{^1\text{H}\}$ (126 MHz) 30.8 (virtual t, $^{49}J_{\text{CP}} = 6.4$ Hz, $\text{PCH}_2\text{CH}_2\text{CH}_2$), 28.6 (s, CH_2), 28.48 (s, CH_2), 28.47 (s, CH_2), 28.4 (s, CH_2), 28.0 (s, CH_2), 27.8 (s, CH_2), 23.9 (s, PCH_2CH_2), 21.5 (virtual t, $^{49}J_{\text{CP}} = 15.9$ Hz, PCH_2), –23.4 (t, $J_{\text{CP}} = 6.5$ Hz, PtCH_3); $^{31}\text{P}\{^1\text{H}\}$ (202 MHz) 8.8 (s, $^1J_{\text{PPT}} = 2824$ Hz).⁴⁸

cis-Pt(Cl)(Me)(P((CH₂)₂₂)₃P) (cis-5g). A. Under air, a round bottom flask was charged with *cis*-4g (0.0664 g, 0.0547 mmol),

CH_2Cl_2 (5 mL). Then HCl (2.0 M in Et_2O , 0.0274 mL, 0.0548 mmol) was added with stirring. After 0.5 h, the solvent was removed by rotary evaporation to give a beige oil containing a *cis*-2g/4g/5g mixture in an approximate 2 : 3 : 5 ratio by ^{31}P NMR, along with other unidentified species. Attempted chromatographic purifications were unsuccessful. *B.* A CH_2Cl_2 solution of crude *cis*-4g (0.2852 g, *ca.* 0.2332 mmol) was chromatographed on neutral alumina (100 : 5 : 1 v/v/v hexanes/ $\text{EtOAc}/\text{Et}_3\text{N}$). The solvent was removed from the product containing fractions (TLC monitoring) by rotary evaporation to give a 18 : 1 mixture of *cis*/*trans*-5g that was *ca.* 80% pure by ^{31}P $\{^1\text{H}\}$ NMR.

Data for *cis*-5e: NMR (CDCl_3 , δ/ppm): ^1H (500 MHz) 1.91–1.68 (br m, 12H, PCH_2), 1.54–1.43 (br m, 12H, PCH_2CH_2), 1.43–1.34 (br m, 12H, $\text{PCH}_2\text{CH}_2\text{CH}_2$), 1.34–1.23 (br m, 96H, remaining CH_2), 0.59 (dd, 3H, $^3J_{\text{HP}(\text{trans})} = 7.0$ Hz, $^3J_{\text{HP}(\text{cis})} = 4.0$ Hz, $^2J_{\text{HPt}} = 49$ Hz, $^{48}\text{CH}_3$); $^{31}\text{P}\{^1\text{H}\}$ (202 MHz) 10.1 (d, $^2J_{\text{PP}} = 12.7$ Hz, $^1J_{\text{Ppt}} = 1739$ Hz, *trans* to CH_3), 3.4 (d, $^2J_{\text{PP}} = 12.7$ Hz, $^1J_{\text{Ppt}} = 4260$ Hz, *cis* to CH_3).

***trans*-Pt(Cl)(Me)(P((CH₂)₂₂)₃P) (*trans*-5g).** *A.* Under air, a vial was charged with *cis*-4g (0.0146 g, 0.0120 mmol), silica gel (0.2572 g), and CH_2Cl_2 (2.5 mL). The mixture was stirred (rt). After 12 h, the sample was filtered and the silica gel further washed with CH_2Cl_2 (25 mL). The solvent was removed from the filtrate by rotary evaporation to give *trans*-5g (0.0118 g, 0.0096 mmol, 80%) as a colorless oil. *B.* A vial was charged with a *ca.* 18 : 1 *cis*/*trans*-5g mixture (0.0350 g, 0.0284 mmol; see preceding paragraph), silica gel (0.9325 g), and CH_2Cl_2 (10 mL). The mixture was stirred (rt). After 12 h, the sample was filtered and the silica gel further washed with CH_2Cl_2 (40 mL). The solvent was removed from the filtrate to give *trans*-5g (0.0224 g, 0.0182 mmol, 64%) as a beige oil. Anal. Calcd for $\text{C}_{67}\text{H}_{135}\text{ClP}_2\text{Pt}$ (1233.26): C, 65.25; H, 11.03. Found: C, 65.53; H, 11.13.

NMR (CDCl_3 , δ/ppm): ^1H (500 MHz) 1.89–1.74 (br m, 12H, PCH_2), 47 1.62–1.47 (br m, 12H, PCH_2CH_2), 1.45–1.35 (br m, 12H, $\text{PCH}_2\text{CH}_2\text{CH}_2$), 1.35–1.18 (br m, 96H, remaining CH_2), 0.31 (t, 3H, $^3J_{\text{HP}} = 6.2$ Hz, $^2J_{\text{HPt}} = 84$ Hz, $^{48}\text{PtCH}_3$); $^{13}\text{C}\{^1\text{H}\}$ (126 MHz) 31.3 (virtual t, $^{49}J_{\text{CP}} = 6.4$ Hz, $\text{PCH}_2\text{CH}_2\text{CH}_2$), 29.4 (s, CH_2), 29.24 (s, CH_2), 29.18 (s, CH_2), 29.1 (s, CH_2), 28.9 (s, CH_2), 28.6 (s, CH_2), 28.5 (s, CH_2), 28.3 (s, CH_2), 24.1 (s, PCH_2CH_2), 21.5 (virtual t, $^{49}J_{\text{CP}} = 15.8$ Hz, PCH_2), –23.1 (t, $J_{\text{CP}} = 6.6$ Hz, PtCH_3); $^{31}\text{P}\{^1\text{H}\}$ (202 MHz) 8.3 (s, $^1J_{\text{Ppt}} = 2796$ Hz).⁴⁸

***trans*-Pt(Br)(Me)(P((CH₂)₁₄)₃P) (*trans*-9c).** A Schlenk flask was charged with *trans*-5c (0.0981 g, 0.1094 mmol), LiBr (0.0488 g, 0.562 mmol) and THF (10 mL). The mixture was stirred (rt). After 12 h, the sample was concentrated and chromatographed on silica gel (3 : 2 v/v hexanes/ CH_2Cl_2). The solvent was removed from the product containing fractions (TLC monitoring) to give *trans*-9c as a colorless oil, which solidified after 1 h (0.0903 g, 0.0960 mmol, 88%), mp (open capillary) 110–119 °C. Anal. Calcd for $\text{C}_{43}\text{H}_{87}\text{BrP}_2\text{Pt}$ (941.08): C, 54.88; H, 9.32. Found: C, 54.99; H, 9.42.

NMR (CDCl_3 , δ/ppm): ^1H (500 MHz) 1.95–1.73 (br m, 12H, PCH_2), 1.66–1.52 (br m, 12H, PCH_2CH_2), 1.48–1.37 (br m, 12H, $\text{PCH}_2\text{CH}_2\text{CH}_2$), 1.37–1.20 (br m, 48H, remaining CH_2), 0.39 (t,

3H, $^3J_{\text{HP}} = 6.1$ Hz, $^2J_{\text{HPt}} = 82$ Hz, $^{48}\text{CH}_3$); $^{13}\text{C}\{^1\text{H}\}$ (126 MHz) 30.1 (virtual t, $^{49}J_{\text{CP}} = 6.8$ Hz, $\text{PCH}_2\text{CH}_2\text{CH}_2$), 28.3 (s, CH_2), 27.4 (s, CH_2), 27.3 (s, CH_2), 26.9 (s, CH_2), 23.5 (s, PCH_2CH_2), 22.5 (virtual t, $^{49}J_{\text{CP}} = 16.0$ Hz, PCH_2), –20.2 (t, $J_{\text{CP}} = 6.4$ Hz, PtCH_3); $^{31}\text{P}\{^1\text{H}\}$ (202 MHz) 8.5 (s, $^1J_{\text{Ppt}} = 2804$ Hz).⁴⁸

***trans*-Pt(I)(Me)(P((CH₂)₁₄)₃P) (*trans*-10c).** Under air, a vial was charged with *trans*-5c (0.0599 g, 0.0668 mmol), NaI (0.0557 g, 0.372 mmol), THF (4 mL) and acetone (4 mL). The mixture was stirred (rt). After 2 d, the sample was concentrated and chromatographed on silica gel (hexanes, then CH_2Cl_2). The solvent was removed from two sets of product fractions (TLC monitoring) to give *trans*-Pt(I)₂(P((CH₂)₁₄)₃P) (0.0077 g, 0.007 mmol, 10%)^{4a} and *trans*-10c (0.0577 g, 0.0584 mmol, 87%) as yellow waxy oils that solidified after 2–4 h, mp (open capillary, *trans*-10c) 114–118 °C. Anal. Calcd for $\text{C}_{43}\text{H}_{87}\text{IP}_2\text{Pt}$ (988.08): C, 52.27; H, 8.88. Found: C, 51.99; H, 8.91.

NMR (CDCl_3 , δ/ppm): ^1H (500 MHz) 2.01–1.88 (br m, 12H, PCH_2), 1.61–1.50 (br m, 12H, PCH_2CH_2), 1.47–1.38 (br m, 12H, $\text{PCH}_2\text{CH}_2\text{CH}_2$), 1.37–1.19 (br m, 48H, remaining CH_2), 0.48 (t, 3H, $^3J_{\text{HP}} = 6.2$ Hz, $^2J_{\text{HPt}} = 81.5$ Hz, $^{48}\text{CH}_3$); $^{13}\text{C}\{^1\text{H}\}$ (126 MHz) 30.1 (virtual t, $^{49}J_{\text{CP}} = 6.6$ Hz, $\text{PCH}_2\text{CH}_2\text{CH}_2$), 28.2 (s, CH_2), 27.4 (s, CH_2), 27.3 (s, CH_2), 26.9 (s, CH_2), 23.9 (br m, PCH_2CH_2), 23.5 (s, PCH_2), –14.8 (t, $J_{\text{CP}} = 6.2$ Hz, PtCH_3); $^{31}\text{P}\{^1\text{H}\}$ (202 MHz) 5.4 (s, $^1J_{\text{Ppt}} = 2767$ Hz).⁴⁸

***cis*-Pt(Et)₂(P((CH₂)₁₄)₃P) (*cis*-6c).** A Schlenk flask was charged with *trans*-2c (0.3018 g, 0.3291 mmol) and Et_2O (15 mL). Then a benzene solution of EtLi (0.5 M, 0.200 mL, 0.100 mmol) was added with stirring (rt). After 12 h, the mixture was exposed to air. After 1 h, the sample was filtered through celite, which was washed with Et_2O (10–20 mL). The solvent was removed from the filtrate by rotary evaporation. The residue was chromatographed on neutral alumina (1 : 0.005 v/v hexanes/ Et_3N). The solvent was removed from the product containing fractions (TLC monitoring) by rotary evaporation. The sample was kept at 4 °C for 2 d but did not solidify, affording *cis*-6c as a colorless oil (0.2524 g, 0.2791 mmol, 85%). Anal. Calcd for $\text{C}_{44}\text{H}_{89}\text{P}_2\text{Pt}$ (988.08): C, 61.10; H, 10.48. Found: C, 60.97; H, 10.70.

NMR (CDCl_3 , δ/ppm): ^1H (500 MHz) 1.84–1.75 (br m, 4H, PCH_2), 1.72–1.50 (br m, 12H), 1.50–1.21 (br m, 68H, remaining CH_2), 1.11–0.81 (br m, 10H, PtCH_2CH_3); $^{13}\text{C}\{^1\text{H}\}$ (126 MHz) 31.1 (virtual t, $^{49}J_{\text{CP}} = 4.2$ Hz, $\text{PCH}_2\text{CH}_2\text{CH}_2$), 30.5 (virtual t, $^{49}J_{\text{CP}} = 6.7$ Hz, CH_2), 28.3 (s, CH_2), 27.5 (s, CH_2), 27.4 (s, CH_2), 26.9 (s, CH_2), 26.8 (s, CH_2), 26.7 (s, CH_2), 26.3 (s, CH_2), 26.1 (s, CH_2), 25.2 (virtual t, $^{49}J_{\text{CP}} = 2.1$ Hz, PCH_2CH_2), 23.2 (s, PCH_2), 23.0 (s, PCH_2), 16.4 (apparent t, $J_{\text{CP}} = 2.1$ Hz, PtCH_2CH_3), 14.8 (dd, $^2J_{\text{CP}(\text{trans})} = 99.8$ Hz, $^2J_{\text{CP}(\text{cis})} = 9.1$ Hz, PtCH_2CH_3); $^{31}\text{P}\{^1\text{H}\}$ (202 MHz) 6.6 (s, $^1J_{\text{Ppt}} = 1746$ Hz).⁴⁸

***trans*-Pt(Cl)(Et)(P((CH₂)₁₄)₃P) (*trans*-7c).** Under air, a round-bottom flask was charged with *cis*-6c (0.3781 g, 0.4181 mmol), CH_2Cl_2 (15 mL), and methanol (1.0 mL). Then CH_3COCl (0.0298 mL, 0.4214 mmol) was added with stirring. After 2 h, the solvent was removed by rotary evaporation. The residue was chromatographed on neutral alumina (5 : 1 : 0.02 v/v/v hexanes/ $\text{Cl}_2\text{CH}_2/\text{Et}_3\text{N}$). The solvent was removed from the product containing fractions (TLC monitoring) by rotary evap-

oration. This gave *trans*-7c as a white solid (0.1727 g, 0.1896 mmol, 45%), mp (open capillary) 119–131 °C. Anal. Calcd for C₄₄H₈₉ClP₂Pt (910.65): C, 58.03; H, 9.85. Found: C, 58.30; H, 10.02.

NMR (CDCl₃, δ/ppm):⁴⁷ ¹H (500 MHz) 1.89–1.78 (br m, 12H, PCH₂), 1.67–1.57 (br m, 12H, PCH₂CH₂), 1.48–1.39 (br m, 12H, PCH₂CH₂CH₂), 1.37–1.24 (br m, 48H, remaining CH₂), 1.18–0.98 (br m, 5H, PtCH₂CH₃); ¹³C{¹H} (126 MHz) 30.1 (virtual t, ⁴⁹J_{CP} = 6.7 Hz, PCH₂CH₂CH₂), 28.3 (s, CH₂), 27.4 (s, CH₂), 27.3 (s, CH₂), 26.9 (s, CH₂), 23.5 (s, PCH₂CH₂), 21.8 (virtual t, ⁴⁹J_{CP} = 15.2 Hz, PCH₂), 18.3 (s, PtCH₂CH₃), –9.6 (t, J_{CP} = 5.4 Hz, PtCH₂); ³¹P{¹H} (202 MHz) 10.5 (s, ¹J_{PPt} = 3002 Hz).⁴⁸

cis-Pt(Cl)(Ph)(P((CH₂)₁₄)₃P) (cis-8c) and trans-8c. Under air, a round bottom flask was charged with *cis*-Pt(Ph)₂(P((CH₂)₁₄)₃P) (*cis*-3c;⁸ 0.0598 g, 0.0598 mmol) and CH₂Cl₂ (6 mL). Then HCl (2.0 M in Et₂O, 0.030 mL, 0.060 mmol) was added with stirring (rt). After 1 h (based upon TLC monitoring), another charge of HCl was added (0.012 mL, 0.024 mmol). After 0.5 h, the solvent was removed by rotary evaporation to give a white solid, which was chromatographed on neutral alumina (first 5:1 v/v hexanes/CH₂Cl₂, then 20:1 v/v hexanes/EtOAc). Two sets of fractions were collected (TLC monitoring). The solvents were removed by rotary evaporation, benzene was added, and the two samples were freeze dried. The first gave *trans*-8c (0.0167 g, 0.0174 mmol, 29%)^{4b} as a white powder; the second gave *cis*-8c (0.0253 g, 0.0264 mmol, 44%) as a white powder, mp (open capillary) 50–55 °C. Anal. Calcd for C₄₈H₈₉ClP₂Pt (958.70): C, 60.14; H, 9.36. Found: C, 60.35; H, 9.48. Data for *trans*-8c agreed with those published earlier.^{4b}

Data for cis-8c: NMR (CDCl₃, δ/ppm):^{47,50} ¹H (500 MHz) 7.39 (m, *o*-Ph, 2H), 7.05 (apparent dt, J_{HH} = 7.3, 1.3 Hz, 2H, *m*-Ph), 6.89 (t, ¹J_{HH} = 7.3 Hz, 1H, *p*-Ph), 2.54–2.42 (m, 2H, PCH₂), 2.03–1.91 (m, 2H, CH₂), 1.90–1.73 (m, 4H, CH₂), 1.72–1.11 (m, 76H, remaining CH₂); ¹³C{¹H} (126 MHz) 136.1 (s, *o*-Ph), 127.93 (s, *m*-Ph), 127.88 (s, *i*-Ph), 112.8 (s, *p*-Ph), 30.93 (s, CH₂), 30.86 (s, CH₂), 30.8 (s, CH₂), 30.7 (s, CH₂), 30.6 (s, CH₂), 30.4 (s, CH₂), 30.3 (s, CH₂), 27.6 (s, CH₂), 27.43 (s, CH₂), 27.37 (s, CH₂), 27.3 (s, CH₂), 27.14 (s, CH₂), 27.11 (s, CH₂), 27.0 (s, CH₂), 26.94 (s, CH₂), 26.93 (s, CH₂), 26.5 (s, CH₂), 26.4 (s, CH₂), 26.3 (s, CH₂), 26.24 (s, CH₂), 25.21 (s, CH₂), 25.19 (s, CH₂), 24.8 (s, CH₂), 23.7 (s, CH₂), 23.4 (s, CH₂), 23.2 (s, CH₂), 23.0 (s, CH₂); ³¹P{¹H} (202 MHz) 5.8 (d, ²J_{PP} = 14.0 Hz, ¹J_{PPt} = 1671 Hz,⁴⁸ *trans* to Ph), 0.2 (d, ²J_{PP} = 14.0 Hz, ¹J_{PPt} = 4228 Hz,⁴⁸ *cis* to Ph).

cis-Pt(Ph)₂(P((CH₂)₁₄)₃P) (cis-3c) and trans-3c. A. A Schlenk flask was charged with *trans*-2c (0.1915 g, 0.2088 mmol)^{4a} and Et₂O (20.0 mL). Then PhLi (1.8 M in Bu₂O, 0.235 mL, 0.423 mmol) was added dropwise with stirring (rt). After 12 h, the mixture was exposed to air. After 1 h, the sample was filtered through celite, which was washed with diethyl ether (20 mL). The solvent was removed from the filtrate by rotary evaporation. The residue was chromatographed on silica gel (first 8:1 v/v hexanes/CH₂Cl₂, then 2:1 v/v hexanes/CH₂Cl₂). The solvent was removed from two sets of product containing fractions (TLC monitoring) by rotary evaporation to give *trans*-

3c (0.1036 g, 0.1036 mmol, 50%) and *cis*-3c (0.0602 g, 0.0602 mmol, 29%) as white solids. The NMR data for each product agreed well with those published earlier.^{4a,8} B. A Schlenk flask charged with *trans*-2c (0.2232 g, 0.2434 mmol)^{4a} and Et₂O (20.0 mL). Then PhLi (1.8 M in Bu₂O, 0.300 mL, 0.540 mmol) was added dropwise with stirring (rt). After 12 h, the mixture was exposed to air. After 1 h, the sample was filtered through celite, which was washed with diethyl ether (20 mL). The solvent was removed from the filtrate by rotary evaporation. The residue was chromatographed on silica gel (8:1 v/v hexanes/CH₂Cl₂). The solvent was removed from product containing fraction (TLC monitoring) by rotary evaporation to give *trans*-3c (0.2077 g, 0.2076 mmol, 85%).

Thermolyses (Table 3 and Scheme 9)

NMR tubes were charged with the following materials and kept at the indicated temperature except for brief intervals when spectra (δ/ppm) were recorded.

Entry 1. *cis*-2c (0.0086 g, 0.0094 mmol or 0.0096 g, 0.0104 mmol), silica gel (0.0925 g), toluene-*d*₈ or CDCl₃ (0.6 mL), 25 °C, 24 h. ³¹P{¹H} NMR 4.5 or 4.8 (s, ¹J_{PPt} = 3498 or 3548 Hz,⁴⁸ *cis*-2c, >99%).

Entry 2. *cis*-3c (0.0070 g, 0.0070 mmol), toluene-*d*₈ (0.7 mL), 80 °C, 10 h. ³¹P{¹H} NMR 4.9 (s, ¹J_{PPt} = 1762 Hz,⁴⁸ *cis*-3c, >99%).

Entry 3. *cis*-3c (0.0090 g, 0.0090 mmol), mesitylene (0.6 mL), 140 °C, 30 h. ³¹P{¹H} NMR 7.4 (s, unknown, 84%), 4.3 (s, unknown, 16%).²⁰ Spectra taken after 1.5–12 h showed additional minor signals.

Entry 4. *cis*-3c (0.0059 g, 0.0059 mmol), silica gel (0.0927 g), toluene-*d*₈ (0.6 mL), 25 °C, 5 h and then 80 °C, 24 h. ³¹P{¹H} NMR 0.5 (s, ¹J_{PPt} = 1760 Hz,⁴⁸ *cis*-3c, >99%).

Entry 5. *cis*-4c (0.0062 g, 0.0068 mmol), toluene-*d*₈ (0.7 mL), 80 °C, 10 h. ³¹P{¹H} NMR 7.3 (s, ¹J_{PPt} = 1868 Hz,⁴⁸ *cis*-4c, >99%).

Entry 6. *cis*-4c (0.0081 g, 0.0092 mmol), mesitylene (0.6 mL), 140 °C, 30 h. ³¹P{¹H} NMR 13.6 (s, unknown, 8%), 10.8 (unknown, 2%), 9.3 (s, unknown, 6%), 7.3 (s, ¹J_{PPt} = 1865 Hz,⁴⁸ *cis*-4c, 84%).

Entry 7. *cis*-4c (0.0071 g, 0.0081 mmol), silica gel (0.1096 g), toluene-*d*₈ (0.6 mL), 25 °C, 24 h. ³¹P{¹H} NMR 7.3 (s, ¹J_{PPt} = 1870 Hz,⁴⁸ *cis*-4c, >99%).

Entry 8. *cis*-4c (0.0072 g, 0.0082 mmol), silica gel (0.0927 g), toluene-*d*₈ (0.6 mL), 25 °C, 5 h (little conversion) and then 80 °C, 24 h. ³¹P{¹H} NMR 11.4 (s, unknown, 76%), 6.2 (s, unknown, 24%).²⁰

Entry 9. *cis*-5c (0.0061 g, 0.0068 mmol), toluene-*d*₈ (0.7 mL), 80 °C, 10 h. ³¹P{¹H} NMR 11.3 and 5.0 (2 d, ²J_{PP} = 11.5 Hz/¹J_{PPt} = 1736 Hz⁴⁸ and ²J_{PP} = 11.5 Hz/¹J_{PPt} = 4167 Hz,⁴⁸ *cis*-5c, 86%), 11.1 (s, *trans*-5c, 14%). The 72 h experiment was similarly carried out in toluene-*d*₆.

Entry 10. *cis*-5c (0.0143 g, 0.0159 mmol), *o*-C₆H₄Cl₂ (0.6 mL), 100 °C, 3 h. ³¹P{¹H} NMR 10.8 (s, ¹J_{PPt} = 2834 Hz,⁴⁸ *trans*-5c, >99%).

Entry 11. *cis*-**5c** (0.0064 g, 0.0071 mmol), *o*-C₆H₄Cl₂ (0.7 mL), 140 °C, 0.5 h. ³¹P{¹H} NMR 10.8 (s, ¹J_{Pt} = 2834 Hz,⁴⁸ *trans*-**5c**, >99%).

Entry 12. *cis*-**5c** (0.0091 g, 0.0100 mmol), C₆D₅Br (0.6 mL), 110 °C, 7 h. ³¹P{¹H} NMR 11.1 (s, ¹J_{Pt} = 2828 Hz,⁴⁸ *trans*-**5c**, >99%). ¹H NMR 2.00–1.84 (m, 12H, PCH₂), 1.84–1.69 (m, 12H, PCH₂CH₂), 1.61–1.49 (m, 12H, PCH₂CH₂CH₂), 1.49–1.32 (m, 48H, remaining CH₂), 0.54 (t, 3H, ³J_{HP} = 5.5 Hz, ²J_{HPt} = 80 Hz,⁴⁸ PtCH₃).

Entry 13. *cis*-**5c** (0.0059 g, 0.0066 mmol), mesitylene (0.6 mL), 140 °C, 0.5 h. ³¹P{¹H} NMR 10.4 (s, ¹J_{Pt} = 2841 Hz,⁴⁸ *trans*-**5c**, >99%).

Entry 14. *trans*-**5c** (0.0072 g, 0.0080 mmol), mesitylene (0.6 mL), 140 °C, 30 h. ³¹P{¹H} NMR 10.8 (s, ¹J_{Pt} = 2844 Hz,⁴⁸ *trans*-**5c**, 87%), 7.3 (s, unknown, 13%).

Entry 15. *trans*-**7c** (0.0089 g, 0.0098 mmol), mesitylene (0.6 mL), 140 °C, 30 h. ³¹P{¹H} NMR 7.4 (s, ¹J_{Pt} = 2447 Hz,⁴⁸ unknown, >99%).²⁰ Spectra taken after 1.5–18 h showed one main intermediate: ³¹P{¹H} NMR 18.3 (s, ¹J_{Pt} = 2756 Hz⁴⁸); ³¹P NMR (undecoupled): 18.3 (br s, w_{1/2} = 27 Hz, ¹J_{Pt} = 2754 Hz⁴⁸); ¹H NMR –16.78 (t, ²J_{HP} = 13.8 Hz, ¹J_{HPt} = 1254 Hz⁴⁸ referenced to C₆H₃(CH₃)₃ at δ 6.78 ppm).

Entry 16. *cis*-**8c** (0.0075 g, 0.0078 mmol), *o*-C₆H₄Cl₂ (0.6 mL), 100 °C, 6 h. ³¹P{¹H} NMR 7.7 (s, ¹J_{Pt} = 2806 Hz,⁴⁸ *trans*-**8c**, >99%).

Entry 17. *cis*-**8c** (0.0053 g, 0.0055 mmol), *o*-C₆H₄Cl₂ (0.6 mL), 140 °C, 0.5 h. ³¹P{¹H} NMR 7.7 (s, ¹J_{Pt} = 2806 Hz,⁴⁸ *trans*-**8c**, >99%).

Entry 18. *trans*-**8c** (0.0098 g, 0.0100 mmol), mesitylene (0.6 mL), 140 °C, 30 h. ³¹P{¹H} NMR 7.7 (s, ¹J_{Pt} = 2806 Hz,⁴⁸ *trans*-**8c**, >99%).

Scheme 9 (right). *cis*-**4c** (0.0134 g, 0.0153 mmol), C₆D₅Br (0.6 mL), 110 °C, 7 h and then 140 °C, 6 h. ³¹P{¹H} NMR 8.9 (s, ¹J_{Pt} = 2806 Hz, *trans*-**9c**, >99%). ¹H NMR 2.28 (s, 1H, C₆D₅CH₃),⁵¹ 2.03–1.92 (m, 12H, PCH₂), 1.79–1.68 (m, 12H, PCH₂CH₂), 1.59–1.49 (m, 12H, PCH₂CH₂CH₂), 1.49–1.37 (m, 48H, remaining CH₂), 0.61 (t, 3H, ³J_{HP} = 6.0 Hz, ²J_{HPt} = 80 Hz,⁴⁸ PtCH₃).

Scheme 9 (left). *cis*-**4c** (0.0062 g, 0.0071 mmol), *o*-C₆H₄Cl₂ (0.6 mL), 140 °C, 12 h. ³¹P{¹H} NMR 10.8 (s, ¹J_{Pt} = 2834 Hz,⁴⁸ *trans*-**5c**, >99%). A spectrum taken after 1 h showed an additional minor signal at 8.9 (s, unknown).

Crystallography

A. Methanol was slowly added dropwise to an Et₂O solution of *cis*-**4c**. After each drop, the mixture was shaken to redissolve the white precipitate formed. When the precipitate persisted, Et₂O was added to regenerate a homogeneous solution, which was kept at 4 °C. After 3 d, colorless crystals were obtained, and data were collected as outlined in Table 1. Cell parameters were obtained from 45 frames using a 1° scan and refined with 102 005 reflections. Integrated intensity information for each reflection was obtained by reduction of the data frames with the program APEX3.⁵² Lorentz and polarization corrections were applied. Data were scaled, and absorption correction were applied using the program SADABS.⁵³ The space group was

determined from systematic reflection conditions and statistical tests. The structure was solved using XT/XS in APEX3.^{52,54} The structure was refined (weighted least squares refinement on *F*²) to convergence.^{54,55} All non-hydrogen atoms were refined with anisotropic thermal parameters. Hydrogen atoms were placed in idealized positions using a riding model. The atoms C29 through C42 and C23 to C24 exhibited elongated thermal ellipsoids and/or nearby residual electron density peaks. These were successfully modeled by disorder between two positions, with occupancy ratios of 0.64 : 0.36, and 0.81 : 0.19 respectively. Appropriate restraints and/or constraints were applied to keep the bond distances, angles, and thermal ellipsoids meaningful. The absence of additional symmetry and voids were confirmed using PLATON (ADDSYM).⁵⁶ B. Colorless crystals of *trans*-**5c** were obtained in a procedure analogous to that for *cis*-**4c**, but starting from the isomer *cis*-**5c**. Either methanol or ethanol could be used. Data were collected on a crystal from each solvent system and both gave the same structure, which was solved as in A. Two pairs of atoms, Cl1/C1 and C39/C40 exhibited abnormal thermal ellipsoids. These were successfully modeled by disorder between two positions, with occupancy ratios of 0.89 : 0.11 and 0.88 : 0.12 respectively. C. An Et₂O solution of *trans*-**10c** was layered with methanol. After 7 d, data were collected on the yellow blocks as outlined in Table 1. The structure was solved and refined in a manner parallel to that in A. The iodide and methyl ligands (I1, C1) were disordered, but this could be modeled and refined to a 86 : 14 occupancy ratio (I1 and I1a as well as C1 and C1a were constrained to have the same thermal ellipsoids). D. Colorless crystals of *trans*-**7c** were obtained in a procedure analogous to that for *cis*-**4c**. Data were collected and the structure was solved in a manner parallel to that in A. Three independent molecules were found in the asymmetric unit. For one, the carbon atoms of the methylene chains exhibited elongated thermal ellipsoids (C91–C132), suggesting disorder. This could be modeled between two positions with an occupancy ratio of 0.33 : 0.67. Appropriate restraints were used to keep bond distances, angles, and thermal ellipsoids meaningful. However, some thermal ellipsoids associated with the modeled positions remained elongated, suggesting further disorder.

Conflicts of interest

The authors declare no competing financial interest.

Acknowledgements

The authors thank the US National Science Foundation (JAG: CHE-1566601, CHE-1900549; MBH: CHE-1664866) for support and Mr. Zhao Liu for helpful observations.

Notes and references

- 1 G. S. Kottas, L. I. Clarke, D. Horinek and J. Michl, Artificial Molecular Rotors, *Chem. Rev.*, 2005, **105**, 1281–1376.

- 2 D. Dattler, G. Fuks, J. Heiser, E. Moulin, A. Perrot, X. Yao and N. Giuseppone, Design of collective motions from synthetic molecular switches, rotors, and motors, *Chem. Rev.*, 2020, **120**, 310–433.
- 3 A. Ehnborn and J. A. Gladysz, Gyroscopes and the Chemical Literature, 2002–2020: Approaches to a Nascent Family of Molecular Devices, *Chem. Rev.*, 2021, **121**, 3701–3750.
- 4 (a) A. J. Nawara-Hultsch, M. Stollenz, M. Barbasiewicz, S. Szafert, T. Lis, F. Hampel, N. Bhuvanesh and J. A. Gladysz, Gyroscope-Like Molecules Consisting of PdX_2/PtX_2 Rotators within Three-Spoke Dibridgehead Diphosphine Stators: Syntheses, Substitution Reactions, Structures, and Dynamic Properties, *Chem. – Eur. J.*, 2014, **20**, 4617–4637; (b) D. Taher, A. J. Nawara-Hultsch, N. Bhuvanesh, F. Hampel and J. A. Gladysz, Mono- and Disubstitution Reactions of Gyroscope Like Complexes Derived from Cl-Pt-Cl Rotators within Cage Like Dibridgehead Diphosphine Ligands, *J. Organomet. Chem.*, 2016, **821**, 136–141; (c) S. Kharel, H. Joshi, N. Bhuvanesh and J. A. Gladysz, Syntheses, Structures, and Thermal Properties of Gyroscope-like Complexes Consisting of $PtCl_2$ Rotators Encased in Macrocyclic Dibridgehead Diphosphines $P((CH_2)_n)_3P$ with Extended Methylene Chains ($n = 20/22/30$) and Isomers Thereof, *Organometallics*, 2018, **37**, 2991–3000.
- 5 (a) L. Wang, F. Hampel and J. A. Gladysz, “Giant” Gyroscope-Like Molecules Consisting of Dipolar Cl-Rh-CO Rotators Encased in Three-Spoke Stators That Define 25–27-Membered Macrocycles, *Angew. Chem., Int. Ed.*, 2006, **45**, 4372–4375; “Gyroskop-Giganten”: Dipolare Cl-Rh-CO-Rotatoren, umgeben von Statoren aus drei Speichen 25-bis 27-gliedriger Makrocyclen, *Angew. Chem.*, 2006, **118**, 4479–4482; (b) L. Wang, T. Shima, F. Hampel and J. A. Gladysz, Gyroscope-like molecules consisting of three-spoke stators that enclose “switchable” neutral dipolar rhodium rotators; reversible cycling between faster and slower rotating $Rh(CO)I$ and $Rh(CO)_2I$ species, *Chem. Commun.*, 2006, 4075–4077; (c) A. L. Estrada, T. Jia, N. Bhuvanesh, J. Blümel and J. A. Gladysz, Substitution and Catalytic Chemistry of Gyroscope-Like Complexes Derived from Cl-Rh-CO Rotators and Triply trans Spanning Di(trialkylphosphine) Ligands, *Eur. J. Inorg. Chem.*, 2015, **2015**, 5318–5321.
- 6 (a) G. M. Lang, T. Shima, L. Wang, K. J. Cluff, K. Skopek, F. Hampel, J. Blümel and J. A. Gladysz, Gyroscope-Like Complexes Based on Dibridgehead Diphosphine Cages That Are Accessed by Three-Fold Intramolecular Ring Closing Metatheses and Encase $Fe(CO)_3$, $Fe(CO)_2(NO)^+$, and $Fe(CO)_3(H)^+$ Rotators, *J. Am. Chem. Soc.*, 2016, **138**, 7649–7663; (b) G. M. Lang, N. Bhuvanesh, J. H. Reibenspies and J. A. Gladysz, Syntheses, Reactivity, Structures, and Dynamic Properties of Gyroscope-like Iron Carbonyl Complexes Based on Dibridgehead Diarsine Cages, *Organometallics*, 2016, **35**, 2873–2889; (c) G. M. Lang, D. Skaper, F. Hampel and J. A. Gladysz, Synthesis, reactivity, structures, and dynamic properties of gyroscope like iron complexes with dibridgehead diphosphine cages: pre- vs. post-metathesis substitutions as routes to adducts with neutral dipolar $Fe(CO)(NO)(X)$ rotors, *Dalton Trans.*, 2016, **45**, 16190–16204.
- 7 (a) T. Fiedler, N. Bhuvanesh, F. Hampel, J. H. Reibenspies and J. A. Gladysz, Gyroscope like molecules consisting of trigonal or square planar osmium rotators within three-spoked dibridgehead diphosphine stators: syntheses, substitution reactions, structures, and dynamic properties, *Dalton Trans.*, 2016, **45**, 7131–7147; (b) G. D. Hess, T. Fiedler, F. Hampel and J. A. Gladysz, Octahedral Gyroscope-like Molecules Consisting of Rhenium Rotators within Cage-like Dibridgehead Diphosphine Stators: Syntheses, Substitution Reactions, Structures, and Dynamic Properties, *Inorg. Chem.*, 2017, **56**, 7454–7469.
- 8 H. Joshi, S. Kharel, A. Ehnborn, K. Skopek, G. D. Hess, T. Fiedler, F. Hampel, N. Bhuvanesh and J. A. Gladysz, Three-Fold Intramolecular Ring Closing Alkene Metatheses of Square Planar Complexes with *cis* Phosphorus Donor Ligands $P(X(CH_2)_mCH=CH_2)_3$ ($X = -, m = 5-10$; $X = O, m = 3-5$): Syntheses, Structures, and Thermal Properties of Macrocyclic Dibridgehead Diphosphorus Complexes, *J. Am. Chem. Soc.*, 2018, **140**, 8463–8478.
- 9 For example, a variety of data exclude initial ligand (L) dissociation from *trans*-II, ³ including square planar, ^{4a,c,5b,c} trigonal bipyramidal, ⁶ and octahedral ⁷ coordination geometries.
- 10 Interestingly, the energy differences do not vary monotonically. Rather, there is an apparent even/odd alternation with respect to $n/2$ (odd, *trans*-2 9.2–8.5 kcal mol^{−1} more stable; even, *trans*-2 5.8–5.1 kcal mol^{−1} more stable).⁸
- 11 G. K. Anderson and R. J. Cross, Isomerisation Mechanisms of Square-Planar Complexes, *Chem. Soc. Rev.*, 1980, **9**, 185–215.
- 12 D. A. Redfield and J. H. Nelson, Equilibrium Energetics of Cis-Trans Isomerization for two Square-Planar Palladium (II)-Phosphine Complexes, *Inorg. Chem.*, 1973, **12**, 15–19.
- 13 Quantitative solvatochromic polarity values are available for all solvents employed in this study ($CH_2Cl_2 > CHCl_3 > o-C_6H_4Cl_2 > C_6H_5Cl > C_6H_5Br > toluene > mesitylene$): C. Reichardt and T. Welton, *Solvents and Solvent Effects in Organic Chemistry*, Wiley, Weinheim, 4th edn, 2011, pp. 455–456.
- 14 (a) E. L. Eliel and S. H. Wilen, *Stereochemistry of Organic Compounds*, Wiley, New York, 1994, pp. 837–838, and 1208; (b) R. S. Ward, Selectivity versus specificity, *Chem. Br.*, 1991, 803–804.
- 15 S. O. Grim, R. L. Keiter and W. McFarlane, A Phosphorus-31 Nuclear Magnetic Resonance Study of Tertiary Phosphine Complexes of Platinum(II), *Inorg. Chem.*, 1967, **6**, 1133–1137.
- 16 R. Romeo, G. D’Amico, E. Sicilia, N. Russo and S. Rizzato, β -Hydrogen Kinetic Effect, *J. Am. Chem. Soc.*, 2007, **129**, 5744–5755. see the supporting information therein.
- 17 R. Romeo and G. D’Amico, Mechanistic Insight into the Protonolysis of the Pt-C Bond as a Model for C-H Bond

- Activation by Platinum(II) Complexes, *Organometallics*, 2006, **25**, 3435–3446. See the supporting information therein.
- 18 S. Otto, Structure and solution behaviour of cyclooctadiene complexes of platinum(II), *Inorg. Chim. Acta*, 2010, **363**, 3316–3320.
 - 19 (a) R. L. Brainard and G. M. Whitesides, The Mechanism of Thermal Decomposition of *trans*-Chloroethylbis(triethylphosphine)platinum(II), *Organometallics*, 1985, **4**, 1550–1557; (b) M. W. Holtcamp, J. A. Labinger and J. E. Bercaw, Ligand effects on the rates of protonolysis and isotopic exchange for platinum(II) alkyls, *Inorg. Chim. Acta*, 1997, **265**, 117–125.
 - 20 The identities of the unknown thermolysis products are being further investigated, but are beyond the scope of the present study.
 - 21 Dassault Systèmes BIOVIA, Materials Studio 6.0, Dassault Systèmes, San Diego, 2017.
 - 22 (a) A. S. Christensen, T. Kubař, Q. Cui and M. Elstner, Semiempirical Quantum Mechanical Methods for Noncovalent Interactions for Chemical and Biochemical Applications, *Chem. Rev.*, 2016, **116**, 5301–5337; (b) J. J. P. Stewart, Optimization of parameters for semiempirical methods VI: more modifications to the NDDO approximations and re-optimization of parameters, *J. Mol. Model.*, 2013, **19**, 1–32.
 - 23 A. V. Marenich, C. J. Cramer and D. G. Truhlar, Universal Solvation Model Based on Solute Electron Density and on a Continuum Model of the Solvent Defined by the Bulk Dielectric Constant and Atomic Surface Tensions, *J. Phys. Chem. B*, 2009, **113**, 6378–6396.
 - 24 (a) R. Romeo, G. Arena and L. M. Scolaro, Steric and Electronic Factors Influencing the Reactivity of Tertiary Phosphines toward Platinum(II) Complexes, *Inorg. Chem.*, 1992, **31**, 4879–4884; (b) C. H. Suresh and N. Koga, Quantifying the Electronic Effect of Substituted Phosphine Ligands via Molecular Electrostatic Potential, *Inorg. Chem.*, 2002, **41**, 1573–1578.
 - 25 F. Basolo and R. G. Pearson, *Mechanisms of Inorganic Reactions*, John Wiley & Sons, New York, 2nd edn, 1967.
 - 26 C. H. Langford and H. B. Gray, *Ligand Substitution Processes*, W. A. Benjamin, Reading, Massachusetts, 1966.
 - 27 S. Kharel, H. Joshi, S. Bierschenk, M. Stollenz, D. Taher, N. Bhuvanesh and J. A. Gladysz, Homeomorphic Isomerization as a Design Element in Container Molecules; Binding, Displacement, and Selective Transport of MCl₂ Species (M = Pt, Pd, Ni), *J. Am. Chem. Soc.*, 2017, **139**, 2172–2175.
 - 28 M. Stollenz, M. Barbasiewicz, A. J. Nawara-Hultsch, T. Fiedler, R. M. Laddusaw, N. Bhuvanesh and J. A. Gladysz, Dibrigehead Diphosphines that Turn Themselves Inside Out, *Angew. Chem., Int. Ed.*, 2011, **50**, 6647–6651; Dreifach-verbrückte Diphosphane mit von innen nach außen invertierender Konfiguration, *Angew. Chem.*, 2011, **123**, 6777–6781.
 - 29 R. W. Alder and S. P. East, In/Out Isomerism, *Chem. Rev.*, 1996, **96**, 2097–2111.
 - 30 W. J. Louw, Preparative and Kinetic Study on the Mechanisms of Isomerization of Square-Planar Complexes. Kinetic Evidence for Pseudorotation of a Five-Coordinate Intermediate, *Inorg. Chem.*, 1977, **16**, 2147–2160.
 - 31 M. K. Cooper and J. M. Downes, Chelate Complexes of Phosphorus–Nitrogen Ligands. 1. Deprotonation, Cis-Trans Isomerism, and Anion-Catalyzed Isomerization in Platinum(II) Complexes of (*o*-Aminophenyl)diphenylphosphine, *Inorg. Chem.*, 1978, **17**, 880–884.
 - 32 M. S. Holt and J. H. Nelson, Platinum(II) complexes of (cyanoethyl)phosphines, *Inorg. Chem.*, 1986, **25**, 1316–1320.
 - 33 (a) T. Leyssens, D. Peeters, A. G. Orpen and J. N. Harvey, How Important Is Metal-Ligand Back-Bonding toward YX₃ Ligands (Y = N, P, C, Si)? An NBO Analysis, *Organometallics*, 2007, **26**, 2637–2645; (b) H. F. Pérez, P. Etayo, A. Panossian and A. Vidal-Ferran, Phosphine-Phosphinite and Phosphine-Phosphite Ligands: Preparation and Applications in Asymmetric Catalysis, *Chem. Rev.*, 2011, **111**, 2119–2176.
 - 34 The relative σ donor and π acceptor properties of a variety of ligands are treated in this review: B. J. Coe and S. J. Glenwright, Trans-effects in octahedral transition metal complexes, *Coord. Chem. Rev.*, 2000, **203**, 5–80.
 - 35 (a) K. Fagnou and M. Lautens, Halide Effects in Transition Metal Catalysis, *Angew. Chem., Int. Ed.*, 2002, **41**, 26–47; Der Einfluss von Halogenidionen in der Übergangsmetallkatalyse, *Angew. Chem.*, 2002, **114**, 26–49; (b) D. L. Lichtenberger, A. R. Rai-Chaudhuri, M. J. Seidel, J. A. Gladysz, S. K. Agbossou, A. Igau and C. H. Winter, Delocalized Electronic Interactions in Chiral Cyclopentadienylrhodium Halide Complexes. Valence Photoelectron Spectra of CpRe(NO)(L)X (Cp = η^5 -C₅H₅, η^5 -C₅(CH₃)₅; L = CO, P(C₆H₅)₃; X = Cl, Br, I), *Organometallics*, 1991, **10**, 1355–1364.
 - 36 J. Zhu, Z. Lin and T. B. Marder, Trans Influence of Boryl Ligands and Comparison with C, Si, and Sn Ligands, *Inorg. Chem.*, 2005, **44**, 9384–9390.
 - 37 (a) Importantly, the *trans* isomers essentially lack dipole moments, and only solvent corrected gas phase optimized structures were computed. The *cis* isomers, with their much larger dipole moments, would be expected to further optimize their gas phase geometries in the more polar solvents (*versus* a much lesser extent with the *trans* isomers), resulting in additional stabilization (b) It is also worth noting that out of the equilibria in Fig. 5 and 6, the largest *cis/trans* energy differences in toluene (less polar) as compared to *o*-C₆H₄Cl₂ (more polar)¹³ are for the dichloride complexes **2c** and **2''** ($\Delta\Delta G = 4.4$ (7.9 vs. 3.5) and 5.3 (6.1 vs. 0.8) kcal mol⁻¹, respectively). This follows from the higher dipole moments of the *cis* dichloride complexes *versus* the other *cis* complexes.
 - 38 Given that *trans-3c* and *cis-3c* exhibit the second highest gas phase energy difference in Fig. 5, we speculate that additional steric or electronic factors are in play.
 - 39 For a lead reference with many relevant citations, see: E. V. Jones, D. Chen, S. W. Wright, J. I. Trujillo and

- S. France, Elucidation of a Sequential Iminium Ion Cascade Reaction Triggered by a Silica Gel-Promoted Aza-Peterson Reaction, *J. Org. Chem.*, 2020, **85**, 15660–15666.
- 40 T. G. Appleton, H. C. Clark and L. E. Manzer, The *trans*-Influence: Its Measurement and Significance, *Coord. Chem. Rev.*, 1973, **10**, 335–422.
- 41 (a) M. P. Mitoraj, H. Zhu, A. Michalak and T. Ziegler, On the Origin of the *Trans*-Influence in Square Planar d^8 -Complexes: A Theoretical Study, *Int. J. Quantum Chem.*, 2009, **109**, 3379–3386; (b) B. Pinter, V. Van Speybroeck, M. Waroquier, P. Geerlings and F. De Proft, *trans* effect and *trans* influence: importance of metal mediated ligand-ligand repulsion, *Phys. Chem. Chem. Phys.*, 2013, **15**, 17354–17365; (c) A. C. Tsipis, *Trans*-Philicity (*trans*-Influence/*trans*-Effect) Ladders for Square Planar Platinum(II) Complexes Constructed by ^{35}Cl NMR Probe, *J. Comput. Chem.*, 2019, **40**, 2550–2562.
- 42 See for example Table 5.7 of ref. 25.
- 43 For crystal structures of five complexes of the formula *cis*-Pt(Me) $_2$ (PR $_2$ R') $_2$ (R,R' = alkyl or aryl), see: C. M. Haar, S. P. Nolan, W. J. Marshall, K. G. Moloy, A. Prock and W. P. Giering, Synthetic, Structural, and Solution Thermochemical Studies in the Dimethylbis(phosphine) platinum(II) System. Dichotomy between Structural and Thermodynamic Trends, *Organometallics*, 1999, **18**, 474–479.
- 44 Crystal structure of *trans*-Pt(Cl)(Me)(PMePh $_2$) $_2$: M. A. Bennett, H.-K. Chee and G. B. Robertson, Comparison of σ -Alkyl and σ -Perfluoroalkyl Groups as Ligands. 1. Crystal and Molecular Structures of the Methyl-, (Trifluoromethyl)-, and (Pentafluoroethyl)platinum(II) Complexes *trans*-PtClR(PMePh $_2$) $_2$ (R = CH $_3$, CF $_3$, C $_2$ F $_5$), *Inorg. Chem.*, 1979, **18**, 1061–1070.
- 45 Crystal structure of *trans*-Pt(Cl)(Me)(PPh $_3$) $_2$: R. Bardi and A. M. Piazzesi, Crystal and Molecular Structure of *Trans*-(Methyl)chlorobis(triphenylphosphine)platinum(II), *Inorg. Chim. Acta*, 1981, **47**, 249–254.
- 46 K. M. Altus, E. G. Bowes, D. D. Beattie and J. A. Love, Intermolecular Oxidative Addition of Aryl Halides to Platinum(II) Alkyl Complexes, *Organometallics*, 2019, **38**, 2273–2277.
- 47 The ^1H and ^{13}C NMR signals of the dibridgehead diphosphine ligands were assigned by analogy to those in ref. 4 (*trans* complexes) and 8 (*cis* complexes), which were in turn established by 2D NMR experiments.
- 48 This coupling represents a satellite (d, ^{195}Pt = 33.8%) and is not reflected in the peak multiplicity given.
- 49 W. H. Hersh, False AA'X Spin-Spin Coupling Systems in ^{13}C NMR: Examples Involving Phosphorus and a 20-Year-Old Mystery in Off-Resonance Decoupling, *J. Chem. Educ.*, 1997, **74**, 1485–1488. The *J* values represent the distance between adjacent peaks in the apparent triplet.
- 50 The ^1H and ^{13}C NMR signals of the phenyl ligand were assigned based upon ^1H , ^1H COSY and ^1H , ^{13}C HSQC and HMBC experiments.
- 51 Based upon integration, the yield of toluene- d_5 is about 33%.
- 52 APEX3, Bruker AXS Inc., Madison, WI, USA, 2012.
- 53 G. M. Sheldrick, SADABS, Bruker AXS Inc., Madison, WI, USA, 2001.
- 54 (a) G. M. Sheldrick, A short history of SHELX, *Acta Crystallogr., Sect. A: Found. Crystallogr.*, 2008, **64**, 112–122; (b) G. M. Sheldrick, SHELXT – Integrated space-group and crystal-structure determination, *Acta Crystallogr., Sect. A: Found. Adv.*, 2015, **71**, 3–8.
- 55 O. V. Dolomanov, L. J. Bourhis, R. J. Gildea, J. A. K. Howard and H. Puschmann, OLEX2: A Complete Structure Solution, Refinement and Analysis Program, *J. Appl. Crystallogr.*, 2009, **42**, 339–341.
- 56 A. L. Spek, Single-crystal structure validation with the program PLATON, *J. Appl. Crystallogr.*, 2003, **36**, 7–13.